1-1-2016

Novel Design And Synthesis Of Transition Metal Hydroxides And Oxides For Energy Storage Device Applications

Peifeng Li
Wayne State University,

Follow this and additional works at: https://digitalcommons.wayne.edu/oa_theses

Part of the Materials Science and Engineering Commons, Nanoscience and Nanotechnology Commons, and the Oil, Gas, and Energy Commons

NOVEL DESIGN AND SYNTHESIS OF TRANSITION METAL HYDROXIDES AND OXIDES FOR ENERGY STORAGE DEVICE APPLICATIONS

by

PEIFENG LI

THESIS

Submitted to the Graduate School

of Wayne State University,

Detroit, Michigan

in partial fulfillment of the requirements

for the degree of

MASTER IN SCIENCE

2016

MAJOR: Materials Science and Engineering

Approved By:

_____

Advisor   Date

DEDICATION

This thesis is dedicated to my beloved parents Xiyu Li and Haiyan Zhao. Thank you for all of

your support and love.

ACKNOWLEDGEMENTS

First and foremost, I sincerely thank my advisor, Dr. Simon Ng, for his invaluable advice, constant guidance, timely support and continuous encouragement all these years. I have benefited enormously from his innovative research ideas across different disciplines and many in-depth discussions and brainstorms. He has not only shared with his scientific ideas and provided constructive and critical comments, but he has taught me many soft skills including generating scientific ideas based on hypothesis, solving problems from different perspectives and writing papers logically. I would not have been able to finish this master's thesis without his close guidance. I appreciate the methodologies, stories and philosophies he has shared with me. His enthusiasm and dedication to research has partially inspired me to pursue a career in scientific research.

I would also like to acknowledge my committee members, Dr. Mark Cheng, and Dr. Da Deng for their insightful comments and suggestions on my thesis. I gratefully appreciate their valuable time serving on my dissertation committee.

I would like to thank all my lab mates, particularly, Jian Zhu, Zhuolun Tang, Junheng Xing, Wenduo Zeng for their help and friendship. It's sincerely appreciated for your help.

I would like to express my deepest gratitude to my parents and grandparents, for their endless and selfless love. I would not have a chance to pursue and complete my master's thesis without their support and encouragement.

Finally, I would like to thank all the nice persons who have helped me in one way or another during my academic years.

TABLE OF CONTENTS

LIST OF TABLES

LIST OF FIGURES

CHAPTER 1. INTRODUCTION

1.1 Overview of research

Currently, the development of electrical vehicles and consumer electronics was hindered by the energy storage devices, such as energy and power density, cycle life, and safety, etc. Improving and enlarging the application range of electric appliances is in urgent need of the research and development for the next generation energy storage devices. In among of these different electrochemical energy storage/ conversion devices, supercapacitors (SCs) and Li-ion batteries (LIBs) are considered as two of the most promising energy storage technology and have been investigated extensively in the past decade, due to the high power density of SCs and high energy density of LIBs.[1]

1.2 Supercapacitors (SCs)

While electrostatic capacitors have been used as an energy storage device for almost a century, low specific capacitance have limited them to low power applications. Among the myriad electrochemical energy storage/conversion devices, electrochemical capacitors (ECs), also known as supercapacitors (SCs), are attractive since their rapid power delivery and recharging (i.e., high power density).[2]

There are two types of SCs, the electric double layer capacitor (EDLC) and pseudocapacitor. EDLCs store energy by a separation of charge in a Helmholtz double layer, while the storage of the electrical energy in the pseudocapacitor is achieved by reversible surface faradaic redox reactions with charge-transfer.[2]

1.3 Lithium ion batteries (LIBs)

Rechargeable lithium-ion batteries (LIBs) have been considering as power sources for wide range of applications, such as consumer electronic devices and electric vehicles due to good

specific energy, high voltage, longer cycling stability, low self-discharge, as well as minimal memory effect among all the rechargeable batteries.[3] Currently, $LiCoO_2$ or $LiMn_2O_4$/ carbon based materials, have been widely used as cathode/anode materials. However, carbon based materials with limited theoretical specific capacity (372 mA h g^{-1}), and relatively low power density give rise to a very limited energy output for LIBs, which limits the further applications for LIBs as energy storage devices. Therefore, finding alternative anode materials to replace graphite in LIBs with better storage capacity, higher rate capability is more and more important for the LIBs research and development. Recently, nanostructured transition metal oxides have been attracted attention since their advantages of high surface-to-volume ratio and short path length for Li-ion diffusion in comparison with their bulk counterparts, and much higher theoretical capacities as compared to carbon based materials. As a result, the study of high capacity TMOs materials with unique nanostructure has increased significantly.

In addition, most of the reported lithium storage capabilities of transition metal oxides have focused on its use as a cathode materials. The potential of using transition metal oxides as an anode material remain not fully elucidated.

1.4 Challenges of research

With rapid development in personal portable devices and electric vehicles, the demand of energy storage systems with higher energy density, higher power density and longer cycle life are also increasing rapidly.

However, the high theoretical capacitance of monometallic oxides or hydroxides for pseudocapacitors can hardly be achieved due their intrinsic limitations, such as poor electric conductivity, poor electrochemical reversibility, cycling instability, and low rate performance, etc.[2, 4, 5] For instance, $Ni(OH)_2$ has a high specific capacitance （2217 F g^{-1} at 2 A g^{-1}） but

the intrinsic low electrochemical reversibility of $Ni(OH)_2$ causes the poor rate performance.[4] On the other hand, the high cost of some rare metals is another issue. For example, RuO_2 pseudocapacitor has a high theoretical specific capacitance ($\sim$1000F g^{-1}), however RuO_2 is prohibitive in price (It costs more than \$1 million for a vehicle-size SCs).[2] To address these issues, bimetallic oxides/hydroxides, for instance $NiCo_2O_4$,[6] $NiMoO_4$,[7] $CoMoO_4$,[8-10] $MnMoO4$,[11] $MnCo_2O_4$,[12, 13] $CoMn(OH)_4$,[14, 15] $NiMn(OH)_4$,[14, 16] and $CoFe(OH)_5$[17] are emerging recently as novel and promising electrode materials for high-performance supercapacitors. Bimetallic oxides/hydroxides exhibit synergistic effects and minimize the defects of the monometallic component material.[5] Moreover, the multiple oxidation states of multi-metallic compounds could generate higher specific capacitances than single-metallic oxides.[18] For example, $Ni(OH)_2$ suffers from low cyclic stability, poor electric conductivity, and bad rate performance, whereas $NiCo(OH)_4$ possesses high capacitance and excellent cyclic stability.[5] In addition, as compared to mono-/double-metallic hydroxides/oxides, triple hydroxides/oxides may provide further electrochemical improvement by introducing one more metallic components. For instance, in electrocatalyst applications, NiCoFe layered triple hydroxide nanosheets[19] was reported as an electrocatalyst for water splitting and showed improved performance as compared to its mono-/double-metallic components. Similarly, NiMnCo or LiNiMnFeO materials have attracted a lot of attention with their ability to address the intrinsic limitation of $LiCoO_2$ or $LiNiO_2$ for battery applications.[20, 21] However, although tri-metallic compounds exhibit improved electrocatalytic and electrochemical performance as compared to mono-/bi-metallic compounds, the effects of tri-metallic hydroxides on supercapacitor capacitance and durability has not been fully elucidated.

Nanotechnology have been raised up as an effective way to improve the electrochemical energy storage properties of energy storage devices, such as SCs and LIBs. The large surface area to volume ratio, short ion transport pathways, and suitable mesopore distribution can theoretically facilitate the faradaic redox reaction at the surface and promote the mass transfer of electrolytes. For example, nanotubes[7], nanosheets[22-24], nanowire[25, 26], nanosphere[27-29] structures all present a better energy storage performance than macro-/bulk-structures. A facile, fast, environmental friendly, and economical synthesis method to prepare multi-metallic compounds (MMC) with unique nanostructures to further improve the electrochemical performance of materials is still a big challenge.

Recently, lots of progresses have been achieved in the synthesis of multi-metallic oxides/hydroxides, such as in situ growth approach[15], hydrothermal process[17], sonochemical synthesis[30], electrochemical deposition (ECD), etc. Generally, as a synthesis which has potential to be used for industrial application, it needs to meet stricter criteria such as economic efficiency, environmental friendliness. However, the first three mentioned methods couldn't satisfy all the criteria for industry application. For instance, hydrothermal methods require toxic additives, in situ growth route is generally tedious, and the control of products quality is hard to achieve via sonochemical method. As comparison, electrodeposition has been considered as a one-step, environment friendly, and economically efficient electrode preparation technology, which is easily adapt to the batch production for industrial application.

1.5 Significance of research

The improvement of electrochemical energy storage device is a multi-facetted problem, and could be achieved by the improvement of many key components in energy storage system. Based on the methods of preparation and their effect on material structure, this research has gained a

better understanding of Ni-Mo-Co triple hydroxides/oxides on electrochemical performance as below:

This research provides an efficient way to prepare the Ni-Mo-Co triple hydroxides nanoflakes electrodes using in SCs, and as anode materials for LIBs. The morphology (hierarchical nanostructure of materials), the size of composites, as well as the crystallinity of materials can be controlled precisely by the synthesis conditions, and can directly affect the electrochemical performance. Thus, the energy storage materials can be designed and optimized to achieve better electrochemical property by optimizing preparative conditions.

To the best of our knowledge, the effects of mutli-metallic hydroxides on capacitance, electrochemical performance, and durability for energy storage devices have not been fully elucidated. Thus, this research focuses on the study of electrode active materials (both positive electrode for SCs and anode for LIBs) to gain a better understanding of the effect of Ni, Mo and Co composition on the morphology, electrochemical performance of Ni-Co-Mo tri-metallic hydroxides, oxides for the application of SCs and LIBs.

1.6 Scope of the thesis

Given the significance of the SCs and LIBs and the important role of transition metal hydroxides/oxides materials in energy storage devices, our research is focused on the synthesis, materials characterizations as well as their electrochemical performance measurement as SCs and LIBs.

In this thesis, the background, the basic concept, challenges of research as well as the key aspects from which the electrochemical performance of energy storage device can be improved were introduced in Chapter 1.

The fundamental of SCs, including the structure of a SC system, the principle of how SCs work, electrode materials for SCs, separators for supercapacitors, electrolytes for supercapacitors, as well as advantages and limitations of supercapacitor were presented in Chapter 2. Besides, the fundamental of LIBs was also introduced in Chapter 2, including the structure, electrode materials, advantages and limitations of LIBs. The last but not the least, a brief comparison between LIBs and SCs was introduced in Chapter 2 as well.

The details of this research work begin from Chapter 3, which was starting with the experimental section, including the preparation (synthesis) of materials, materials characterization, as well as electrochemical performance measurement/evaluation for materials in the use of SCs and LIBs.

Ni-Mo-Co triple hydroxides (THs) nanoflakes were synthesized by a one-step electrodeposition method based on the Ni-foam substructure. In order to get a better understanding of these materials, XRD, XPS, SEM, TEM were employed (Chapter 4). The morphology and structure and the electrochemical performance of as-prepared samples were discussed in Chapter 4.

Followed by the Ni-Mo-Co THs nanoflakes, the preparation of Ni-Mo-Co triple oxides (TOs) nanoflakes and the electrochemical performance of Ni-Mo-Co TOs nanoflakes as anode electrode materials for LIBs was discussed in Chapter 5. The as-prepared tri-metallic oxides nanoflakes exhibited excellent rate performance and cyclability with high reversible specific capacity of larger than 1000 mA h g^{-1}.

CHAPTER 2. BACKGOROUND

2.1 Fundamentals of supercapacitor (SCs)

2.1.1 What is a supercapacitor

In an ordinary capacitor, it has two plates that are separated and facing each other, energy is stored by means of a static charge as opposed to an electrochemical reaction. And the plates are separated by a relatively conventional thick solid dielectric, such as mica, thin plastic film, or even simply air.
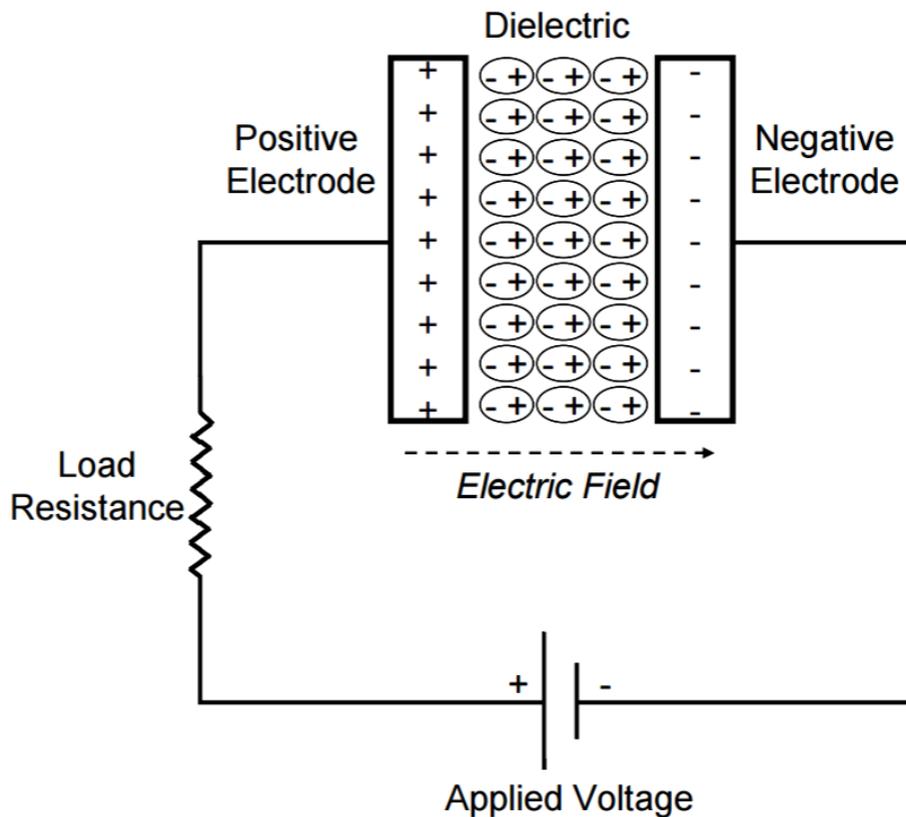
Fig. 2-1-1. The schematic of a conventional capacitor.[31]

As shown in Fig. 2-1-1, when the capacitor is charged up, the positive and negative charges are formed on the two facing plates respectively, creating an electric field between those two plates. In addition, the capacitance of the ordinary capacitor is calculated by the equation:[32]

$$C = \frac{\varepsilon_o \varepsilon_r A}{d}$$

Where C is capacitance (Farads), d is the distance the two electrodes (m), A is the surface area of the two conductive plates (m), ε_o is the dielectric constant (or called "permittivity") of vacuum, ε_r is the constant of insulator. Per this equation, there are three methods to increase the capacitance of conventional capacitor: 1) using insulator with a higher dielectric constant; 2) increasing the surface area of the conductive electrodes; and 3) decreasing the distance between the electrodes.

Differs from an ordinary capacitor, the supercapacitor (SC), also known as electrochemical capacitor (EC) or ultracapacitor (UC), consists of two electrodes separated by a separator, has a much higher specific capacitance, and can store charges with a much bigger area. Moreover, the distance between two electrodes is smaller, since no dielectric layer is needed as conventional capacitor. Instead, both electrodes are soaked in an electrolyte and separated by a very thin insulator. There are three types of supercapacitor, the electric double layer capacitor (EDLC), pseudocapacitor, as well as hybrid capacitor (EDLC plus pseudocapacitor), as shown in Fig 2-1-2.
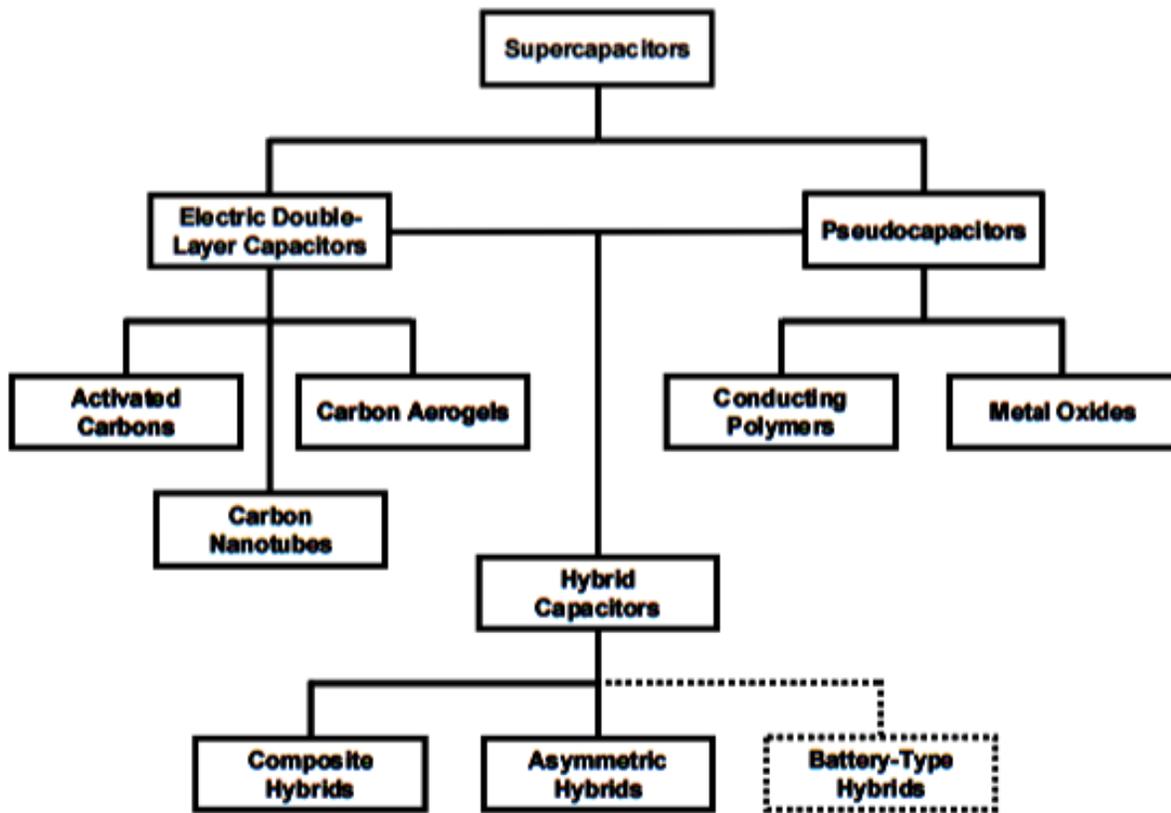
Fig. 2-1-2. The family tree of supercapacitor types. EDLCs, pseudocapacitors, as well as hybrid capacitors.[31]

Electrochemical capacitors represent a new breed of energy storage devices. They can store higher amounts of energy than conventional capacitors, and deliver much more power than most of rechargeable batteries. As such, electrochemical capacitors can bridge the gap between electrolytic capacitors and rechargeable batteries, as shown in the Ragone plot below (Fig. 2-1-3).[33]
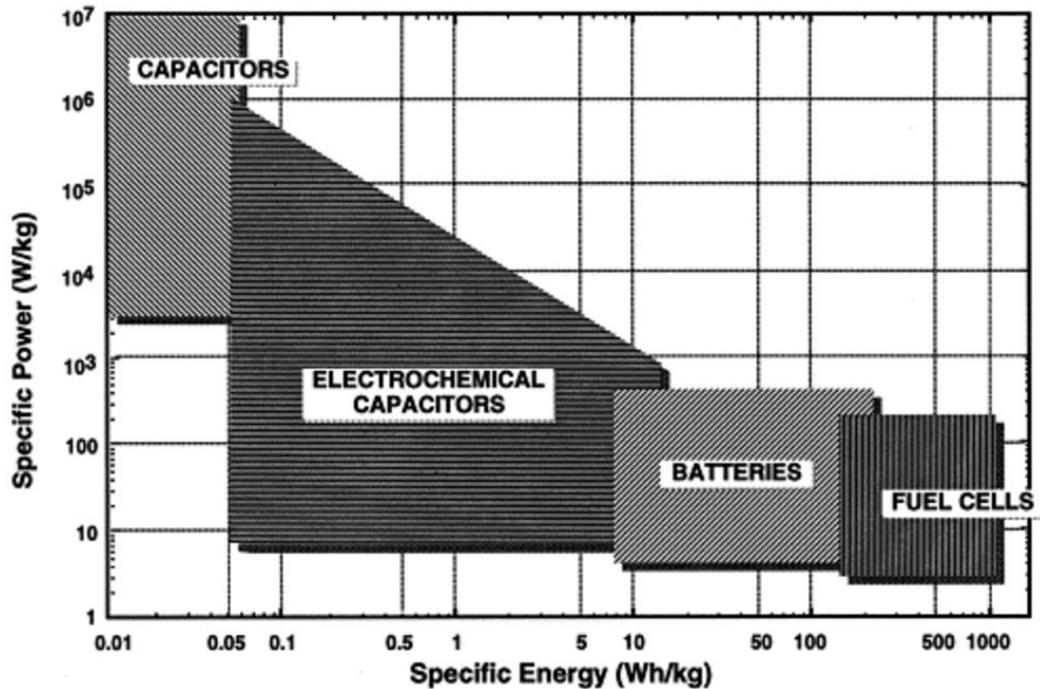
Fig. 2-1-3. The sketch of Ragone plot for various energy storage and conversion devices. The indicated areas are rough guide lines. [33]

For EDLCs, the electrodes are usually carbon-based materials or transition metal hydroxides/oxides, which usually have a high surface area. The distance between two charged surface is the thickness of the Helmholtz double layer. Not like conventional capacitor, which store charges at flat conductor plates, supercapacitor use the double-layer effect to store the energy, which store charges at the interface between the electrode materials and the electrolyte.
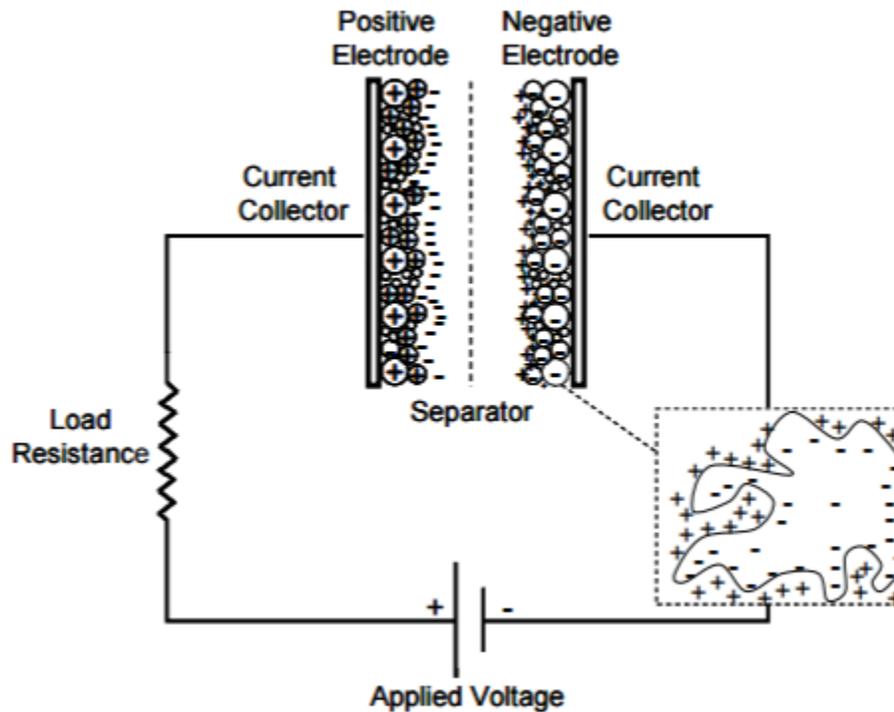
Fig. 2-1-4. The schematic of a EDLC.[31]

There are two ways to store the electric energy in the double-layer of the electrodes that combine as the total capacitance of a supercapacitor:[34] 1. Double-layer capacitance (Fig. 2-1-4), which store energy by a separation of charge in a Helmholtz double layer. In one electrochemical capacitor, two electrodes, separator are ionically connected to each other by the electrolyte with a mixture of positive and negative ions. There are two interface originated on the surface of each electrodes between the electrolyte.[35] When apply a voltage to the electrochemical capacitor, an opposite charge forms on either side of the separator, creating the Helmholtz double layers at the interface between electrolyte and active materials for each electrode, one layer is on the surface of the electrode, and another is emerged from ions in the electrolyte, with an opposite polarity. These two layers are separated by a monolayer of solvent, which is called inner Helmholtz plane (IHP). This solvent "separator" is caused by physical adsorption, without any transfer of charge between electrolyte and electrode. Since the lack of

transfer of charge between electrolyte and electrode, the adhered monolayer is polarized but no chemical changes. After charging, the amount of charge is matched by the large number of counter-charges in outer Helmholtz plane (OHP). The static electric field which is formed by the double-layer charge in the layer of the solvent molecules in the IHP corresponds to the charged voltage. Accordingly, with the equation discussed above for capacitance C, EDLCs have a higher capacitance values than ordinary capacitors, resulting from a higher dielectric constant ε, larger plate surface area A, as well as smaller distance between two electrodes d.

Electrochemical pseudocapacitor store energy via reversible surface faradic redox reaction in charge-discharge.[36-38] During charging process, the very fast reversible redox reaction happened on the surface of suitable electrodes with the electric double-layer. The electron charge-transfer is coming from a de-solvated and adsorbed ion, and since only a charge-transfer happened on the surface of electrode, there is no chemical reaction with the atoms from the electrode. In addition, since the electrons are transferred from/to valence electron states of the redox electrode reagent, the ability of capacitance is depending on the intrinsic property, structure, size of electrode materials. The redox reaction only happened if the applied voltage is higher than the potential of electrode materials, as such, the amount of electric charge stored in pseudocapacitance is related with the applied voltage.

2.1.2 Electrode materials for supercapacitors

Generally, SCs electrodes must have good conductivity, cycling stability, high energy storage capacity, high specific surface area, good rate performance, low cost, as well as environmental friendliness. In addition, the capacitance stored/unit voltage is predominantly a function of the surface area, usually the smaller the pores, the higher the surface area, specific capacitance and energy density. Thus, SCs electrodes are usually have porous structure, which can provide a

higher specific surface area per unit volume. Additionally, the performance of faradaic charge transfers of electrode materials is also predominantly affect the pseudocapacitance as well.

2.1.2.1 Electrode materials for EDLCs

In the early of 1950s, engineers from General Electric began exploring with porous carbon electrodes for capacitors, and they found that the porous carbon is a good candidate electrode for capacitors. Since then, many high surface area carbon-based materials have been used as the electrode materials, due to their good potential.

Table 2-1 Properties and characteristics of various carbon and carbon-based materials as EDLCs electrode materials[39]

Materials	Specific surface area/m^2 g^{-1}	Density/g cm^{-3}	Aqueous electrolyte		Organic electrolyte	
			/F g^{-1}	/F cm^{-3}	/F g^{-1}	/F cm^{-3}
Carbon materials						
Commercial activated carbons (ACs)	1000–3500	0.4–0.7	< 200	< 80	< 100	< 50
Particulate carbon from SiC/TiC	1000–2000	0.5–0.7	170–220	< 120	100–120	< 70
Functionalized porous carbons	300–2200	0.5–0.9	150–300	< 180	100–150	< 90
Carbon nanotube (CNT)	120–500	0.6	50–100	< 60	< 60	< 30
Templated porous carbons (TC)	500–3000	0.5–1	120–350	< 200	60–140	< 100
Activated carbon fibers (ACF)	1000–3000	0.3–0.8	120–370	< 150	80–200	< 120
Carbon cloth	2500	0.4	100–200	40–80	60–100	24–40
Carbon aerogels	400–1000	0.5–0.7	100–125	< 80	< 80	< 40
Carbon -based composite materials						
TC–RuO$_2$ composite	600	1	630	630	—	—
CNT–MnO$_2$ composite	234	1.5	199	300	—	—
AC–polyaniline composite	1000	—	300	—	—	—

So far, carbon-based materials in various manifestations,[39] such as activated carbon (AC),[31, 38] active carbon fiber (ACF),[40] carbon aerogel,[41] carbide-derived carbon (CDC),[42] graphene,[43, 44] as well as carbon nanotubes (CNTs),[45] were used as electrode materials for the EDLCs due to their superior mechanical and electronic properties as well as relative low cost and high cycle life features.[1] However, the very limited charge storage capability and energy density with carbon-based materials can hardly meet the customers demand as a commercial product and impede their potential for further applications. This is because the capacitance is due to the electrosorption of ions on porous carbon electrodes.[46, 47]

Additionally, the specific capacitance of carbon-based materials is no more than 150 F g^{-1}.[48] As a result, the study regarding nanostructure and pore size of EDLCs electrodes is much more important than the material itself.

2.1.2.2 Electrode materials for pseudocapacitors

However, the very limited charge storage capability and energy density with EDLCs cannot meet the stringent requirement of energy intensive applications. This is because the electric energy is stored between the electrode and electrolyte interface only. [46, 47] On the other hand, pseudocapacitors turns to be a promising approach to address the low energy density of EDLCs. As a qualified electrode for the pseudocapacitor, since the charge storage originates from electron-transfer mechanisms but not the total number of ions in the double layer. They are supposed to have the electrochemical signature of a capacitive electrode and the materials should have a good faradaic behavior. Accordingly, more and more researches were focused on transition metal oxides/hydroxides, such as $Ni(OH)_2$[49, 50], $Co(OH)_2$[51], NiO[22], CoO[52, 53], Co_3O_4[23], RuO_2[54], MnO_2[24], and Fe_3O_4[55] have gained increased interests as pseudocapacitive materials for the next generation of energy storage devices, owing to their high theoretical specific capacitance. Xue et al. showed by synthesizing $Co(OH)_2$ nanowire using a dual-template method, a specific capacitance of 993 F g^{-1} at the current density of 1A g^{-1} was observed. Hu and co-workers[4] have reported that $Ni(OH)_2$ pseudocapacitive material show a high specific capacitance of 2217 F g^{-1}, but it suffer from the low rate performance. The capacitance of those pseudocapacitive materials are much higher than those of EDLC electrode materials, such as carbon-based materials, which only has a capacitance of no more than 150 F g^{-1}.[48]

Besides metal oxides/hydroxides, conductive polymers such as polyaniline, polyacene, polyacetylene, and polythiophene are other materials as the electrodes for pseudocapacitors.[56] The charging/discharging on such electrodes are processed by the electrochemical doping or dedoping of polymers with anions and cations. However, they are generally suffer from limited cycling stability.[57]

2.1.3 Separators for supercapacitors

The usage of a separator in supercapacitor is physically separate the two electrodes to prevent a short circuit by direct contact. It should meet some of following requirements: 1). It should be porous to the conducting ions to allow ions in the electrolyte get through to balance the charges during the charge-discharge process; 2). To make the electrolyte and electrodes stable, resulting in the good property of supercapacitors. Separators must be chemically inert to protect the electrodes, electrolyte's conductivity as well as stability; and 3). Low cost and environment friendliness.

In general, nonwoven porous polymer-based films, such as Kapton, polyacrylonitrile, porous woven ceramic fibres, as well as woven glass fibers, are widely used as a separator in supercapacitors.[58, 59]

2.1.4 Electrolytes for supercapacitors

In supercapacitors, the usage of electrolytes is electrically connecting between the electrodes on each side. To make the electrolytes electrically conductive, they should include both solvent and dissolved chemicals to split into positive cations and negative anions. In addition, the electrolyte can also provide the molecules to build up the monolayer as the inner Helmholtz plane (IHP), as well as transfer the ions for pseudocapacitor.

Traditionally, aqueous electrolytes include KOH alkaline electrode (usually 1M KOH), HNO_3, and H_2SO_4 acidic electrolyte are widely used in supercapacitors, since they are easier to go through the micropores on the surface of electrodes and their good electrically conductivity.[60] Additionally, salt electrolytes, such as KCl, KBr, as well as KNO_3 are also studied.[61]

Compared with aqueous electrolytes, organic electrolytes with organic solvents such as propylene carbonate,[62] acetonitrile,[63] can provide a higher dissociation voltage, as well as a higher temperature range, resulting in a higher energy density directly. However, usually the organic electrolytes contain larger molecules which may lower the mobility of the electrolytes, resulting in increasing the impedance of SCs. In addition, the higher price and lower electrical conductivity of organic solvent limit their use as electrolyte in SCs.

2.1.5 Advantages and limitations of supercapacitors

The major advantages and limitations of SCs are listed in Table 2-2. The high specific power plus specific energy of commercial SCs make them bridge the gap between electrolytic capacitors and rechargeable batteries. Besides, they can store 10-100 times more energy per unit volume than conventional capacitors, can charge and discharge much faster than batteries. In addition, since SCs do not rely on chemical changes in the electrodes, usually SCs have a better cycling stability. Their broad temperature range offers as another advantage over batteries, enabling their use in a wide variety of applications.

Table 2-2 Advantages and Limitations of SCs

Advantages	Limitations
1. Virtually unlimited cycle life	1. Higher self-discharge

Advantages	Limitations
2. High power density	2. Lower specific energy than batteries
3. Low resistance enables high load currents	3. Low working voltage
4. No end-of-charge termination required	4. Higher cost than barriers
5. Overcharge won't affect the energy storage device in a negative way	5. Linear discharge voltage prevents using the full energy spectrum
6. Safe (forgiving if abused)	
7. Excellent low-temperature charge and discharge performance	

However, they suffer from the higher self-discharge rate than most batteries, low cell voltage, which requires series connections with voltage balancing, as well as higher cost per watt than most commercial batteries.

2.2 Fundamentals of Lithium-ion batteries (LIBs)

2.2.1 What is a Lithium-ion battery

Primary Li batteries became as a commercial product during the 1970s.[64] Lithium-ion batteries (LIBs) were first commercialized by Sony and Asahi Kasei in June 1991 and now are widely being used for portable electronic. Due to their high energy density, low self-discharge property, and minimal memory effect,[65, 66] they are one of the most commonly types of rechargeable batteries for portable devices. Beyond these, LIBs are also popular in the field of electric vehicle (EV), military, and aerospace applications.

Just like every electrochemical battery, LIB consists of three primary functional components: positive electrode (cathode), negative electrode (anode), as well as electrolyte. LIB, which is different from non-rechargeable lithium battery (use metallic lithium as one electrode), uses an

intercalated lithium compound as one electrode material, is a type of rechargeable battery. Li-ions move from the anode electrode to the cathode electrode while discharging and back to anode electrode during charging, so LIBs are called rocking chair like batteries since the Li-ions "rock" forth and back between the cathode and anode electrodes when the cell is charged and discharged. Fig. 2-2-1 shows the basic principle of LIB system, the main reactions are reversible Li-ions intercalation-de intercalation cycles, which means Li-ions could move in and out of both electrodes. To maintain anodic stability of both the cathode material and electrolyte, $LiCoO_2$ is often employed as cathode electrode. The reaction of cathode is shown in equation (1):

(1) Li^+ deintercalation/intercalation reaction mechanism:

$$LiCoO_2 \leftrightarrow x\ Li^+ + x\ e^- + Li_{1-x}CoO_2\ (1)$$
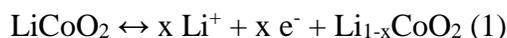
The first process of LIB is always charging, which is called delithiation and oxidation of $LiCoO_2$. Meanwhile, the lithiation and reduction reaction happens on anode electrode, which is graphite in our example. After intercalating with Li ions, it forms to LiC_6, as shown in equation (2):

(2) Li^+ insertion/extraction reaction mechanism:

$$C_6 + Li^+ + e^- \leftrightarrow LiC_6\ (2)$$
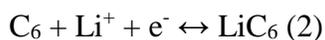
When the battery is in the charge cycle, an electrical power source (also called charging circuit) applies an over-voltage (as the same polarity of charging), forcing a charging current to flow within the battery in the direction of cathode (positive) to anode (negative) electrode. When battery is in the discharge cycle, the Li-ion (Li^+) carry the current within the battery extract from anode electrode (e.g. LiC_6 as below), through the non-aqueous electrolyte and separator diaphragm, and intercalate into the cathode electrode. When the battery is charged, the direction of flow of ions and electrons reverse.[64, 67]
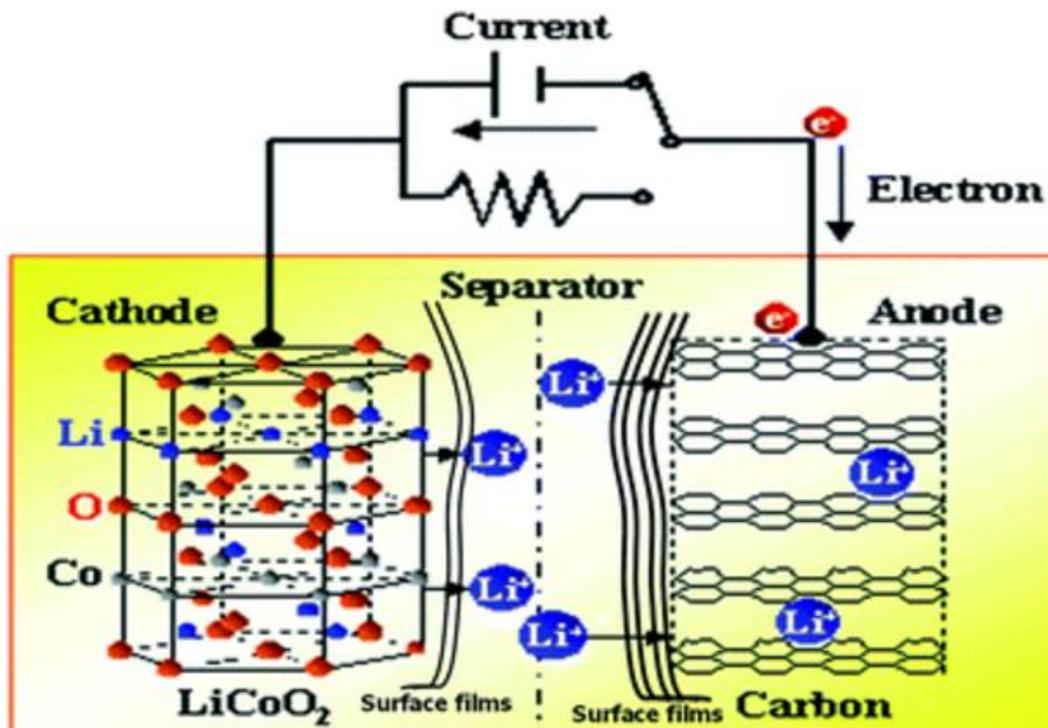
Fig. 2-2-1. The schematic of the most commonly used LIB based on LiC_6 anode electrodes and $LiCoO_2$ cathode electrodes.[64]

It is worth to note that during charge-discharge process, the Li-ions are transported from and to the anode or cathode electrode by oxidizing the transition metal in cathode electrode. For example, cobalt (Co), oxidized from Co^{3+} and Co^{4+} to in $Li_{1-x}CoO_2$ while charging, and reduced from Co^{3+} and Co^{4+} during discharge.

2.2.2 Electrodes for LIBs

2.2.2.1 Positive electrodes (cathodes) for LIBs

From the early stages of R&D of LIBs, transition metal oxides and sulfides are found to be remarkable cathode materials for LIBs.[68] Each Li-ion battery has to contain the Li source, the cathode material (Li_xMO_2), to provide Li-ions and the charge. Table. 2-3 illustrates the characteristic of representative positive electrode materials for LIBs.[69]

Table 2-3 Characteristic of representative positive electrode materials for LIBs[69]

Positive electrode material	Molecular weight	Density [kg/L]	Reversible range Δx	Theoretical specific charge [Ah/kg]	Theoretical charge density [Ah/L]
Charged					
TiS_2	112.01	3.27	1	239	782
MoS_2	160.06	5.06	0.8	134	678
V_2O_5	181.88	3.36	1	147	495
V_6O_{13}	513.64	3.91	3.6	188	734
MnO_2	86.94	5.03	0.5	154	775
$NbSe_3$	329.81	8.7	3	244	2121
Discharged					
$LiCoO_2$	97.87	5.16	0.5	137	706
$LiNiO_2$	97.63	4.78	0.7	192	919
$LiMn_2O_4$	180.82	4.28	1	148	634

Cathode materials are commonly used with two general materials: $LiCoO_4$ (LCO) and $LiMn_2O_4$ (LMO). The LCO cathode materials are attractive since their high specific capacity, minimal self-discharge, high charge applied voltage, as well as good cycling stability. However, LCO suffers from their high cost and environment unfriendliness. By contrast, LMO cathode materials are ideal due to the low price of manganese and environment friendliness. However, the limitations are their poor cycling stability.

In addition, there are other materials which can be used as a cathode electrode material in LIBs. For instance, Lithium Nickel Manganese Cobalt Oxide (i.e. NMC),[20, 70, 71] Lithium Iron Phosphate (i.e. LFP, or $LiFePO_4$),[72, 73] among others.

2.2.2.2 Negative electrodes (anodes) for LIBs

Table. 2-4 illustrates the characteristic of representative negative electrode materials for LIBs.[69] Anode materials are commonly constructed from carbon-based materials, such as graphite. These materials are being widely used since they are abundant, low cost, electrically conducting, as well as have a high-energy density (theoretical specific capacitance, 372 mA h g^{-1}, corresponding to LiC_6). It is worth noting that swelling modestly of anode electrode can accommodate the Li-ions associated with building charge. As such, silicon-based materials have

been attracted a significant research interests, and can store more than 10 times of Li-ions than

carbon-based materials.

Table 2-4 Characteristic of representative negative electrode materials for LIBs[69]

Negative electrode material	Molecular weight		Density [kg/L]		Theoretical specific charge [a] [Ah/kg]		Theoretical charge density [a] [Ah/L]	
Li (primary)	6.94		0.53		3862		2047	
Li$_4$ (secondary)	27.76		0.53		965		511	
LiC$_6$ (graphite)	79.00	(72.06)	2.24	(2.25)	339	(372)	759	(837)
LiAl	33.92	(26.98)	1.75	(2.70)	790	(993)	1383	(2681)
Li$_{21}$Sn$_5$	739.31	(593.55)	2.55	(7.28)	761	(948)	1941	(6901)
LiWO$_2$	222.79	(215.85)	11.30	(12.11)	120	(124)	1356	(1502)
LiMoO$_2$	134.88	(127.94)	6.06	(6.47)	199	(209)	1206	(1352)
LiTiS$_2$	118.94	(112.01)	3.06	(3.22)	225	(239)	689	(782)

However, if the swelling of materials is much more than its limits, it can break the electrical

contacts in the anode electrode, and shut down the Li-ion battery. In addition, as silicon based

anode material, the cracks can be created in the material during the insertion and extraction of

Li-ions, resulting in a thicker SEI layer on the anode surface (Si) after cycles, and lower capacity

and cycling stability.

Recently, nanostructured transition metal oxides have been attracted broad attention as the

potential anode materials,[74, 75] due to their high energy storage capacity as well as high

surface-to volume ratio, and short path length for Li-ion diffusion in comparison with their bulk

counterparts.

2.2.3 Advantages and limitations of LIBs

The major advantages and limitations of LIBs are listed above in Table 2-5. LIBs can

become to one of the most popular energy devices due to the high specific energy (ca. 240 Wh

kg^{-1}) and high energy density (ca. 640 Wh L^{-1}). Besides, the relatively low self-discharge rate (2 %

- 8 % / month, less than half that of nickel-based batteries), high coulombic efficiency (up to

almost 99 %), as well as almost no memory effect, enabling their use in a wide variety of applications.

Table 2-5 Advantages and Limitations of LIBs

Advantages	Limitations
1. High energy density and design flexibility	1. Subject to aging, even if not in use
2. Relatively long cycle stability	2. Transportation restriction
3. Satisfactory coulombic efficiency	3. Expensive to manufacture
4. Relatively low self-discharge effect	4. Not fully mature
5. Low maintenance required	5. Unsafe under a rapidly charging at low-temperatures (less than 0 °C)
6. Rapid charge capability	
7. Almost no memory effect	6. May become unsafe if its over-charged and over-discharge
8. High temperatures range for working and operation	
9. Higher cell voltage	

Table 2-6 and Fig. 2-2-2 show the comparison of different battery technologies in terms of volumetric and gravimetric energy density. As shown in Fig. 2-2-2, without the unsafe Li metal, compared with lead-acid (Pb-acid) batteries, nickel-cadmium (Ni-Cd) batteries, as well as nickel-metal hydride (Ni-MH) batteries, LIBs show a higher density for both volumetric and gravimetric. In addition, in Table 2-6, except lower cycle life at 80 % DOD than Ni-Cds and Ni-MHs, LIBs present a higher cell voltage (twice higher than Ni-Cds and Ni-MHs), no memory effect, less aging effect, as well as higher energy density (at least two times higher than Ni-Cds and Ni-MHs).

Table 2-6 General Secondary Battery Comparison for Consumer Application[76]

Characteristic	NiCd	NiMH	Lithium-Ion
Cell voltage	1.2	1.2	3.6-3.7
Cycle life at 80% DOD	1000+	500+	400-500
Temperature range	−40 to 70°C	−40 to 50°C	−20 to 60°C
Memory effect	Yes	Yes	No
High rate discharge	10C +	Up to 5C	Up to 2C (typical)
Fast charge time	<1 h	2 h	2 h
Capacity after 1 year storage @ 25°C	<30%	<20%	80%
Energy density @ 10 h discharge rate	60 Wh/kg	90 Wh/kg	230 Wh/kg
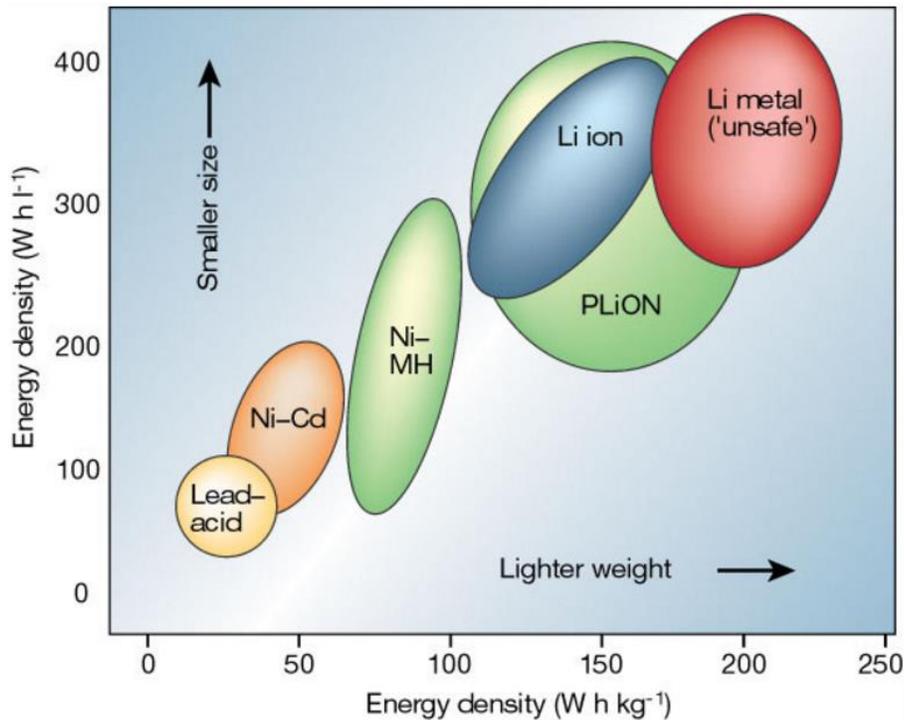
Fig. 2-2-2. The comparison of the different batteries in terms of volumetric and gravimetric energy density.[77]

However, LIBs also suffer from aging issue (storage in a cool place at 40 % charge reduces the aging effect, high produce price, as well as some safety issues while rapidly discharging at low temperature and over- charge/discharge, thus LIBs are still not fully mature so far.

2.3 Comparison of LIBs and SCs

The comparison of potential change during the degree of charge/discharge of LIBs and SCs is showed in Fig. 2-3-1. [78] The cell voltage on a SC decreases linearly, while LIB remains constant. Accordingly, the energy stored in LIB is proportional to the voltage, but for SC, the energy is proportional to the voltage squared. Besides, for SCs, the voltage provides a convenient measure of the amount of state of charge (SOC), however, not for LIBs.
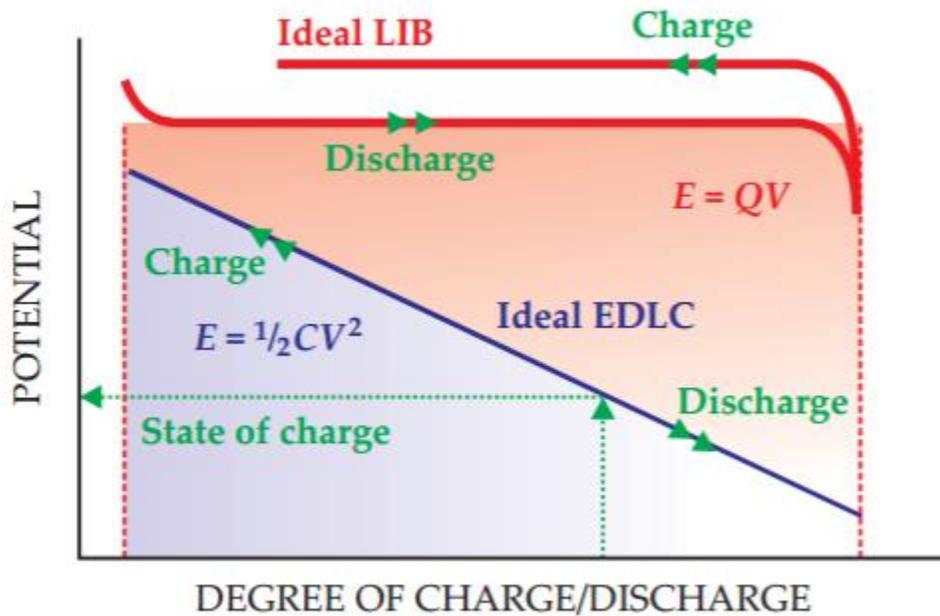
Fig. 2-3-1. Comparison potential change during the degree of charge/discharge of LIBs and SCs.[78]

Table 2-7 shows the comparison of properties of rechargeable batteries and electrochemical capacitors.[2] The storage mechanism for rechargeable batteries is chemical reaction while the ECs is physical (electric double layer). The power limitation of battery is reaction kinetics, mass transport, whereas for ECs is electrolyte conductivity. The energy stored in a battery is usually higher than a EC per unit volume, since the bulk of electrode is storing energy while the energy just stores on the surface area in a EC. Besides, ECs have a higher rate performance, and usually longer cycle life than rechargeable batteries.

Table 2-7 Comparison of properties of rechargeable batteries and electrochemical capacitors (ECs)[2]

Property	Battery	Electrochemical capacitor
Storage mechanism	Chemical	Physical
Power limitation	Reaction kinetics, mass transport	Electrolyte conductivity
Energy storage	High (bulk)	Limited (surface area)
Charge rate	Kinetically limited	High, same as discharge rate
Cycle life limitations	Mechanical stability, chemical reversibility	Side reactions

2.4 Summary of the background

As a summary of aforementioned background review, the fundamental of SCs and LIBs, including the main structures of SCs and LIBs, electrode materials, separators, electrolytes, advantages & limitations of studied energy storage devices, as well as energy storage principle/mechanism, were discussed.

Based on the background review of SCs and LIBs, it's clear that not only the intrinsic properties of materials, the materials size (either in nano- or in micro-scale), but the hierarchical structure and composition of materials can affect the electrochemical performance of active materials. Herein, the overall objective of this research is to gain a better understanding on the effect of composition of Ni-Mo-Co triple hydroxides/oxides positive/anode materials on the electrochemical performance in SCs and LIBs.

CHAPTER 3. EXPERIMENTAL SECTION

3.1 Preparation of Ni-Mo-Co hydroxides nanoflakes

In a typical procedure, all chemicals were of reagent grade quality and were used without further purification. The Ni foam (10x10mm for SCs and 7 x 7mm for LIBs) was ultrasonically cleaned with 2M HCl, ethanol, deionized (DI) water consequently, and dried in vacuum oven for 24h before electrodeposition. The electrodeposition of Ni-Mo-Co triple hydroxides (THs) were performed in a standard three-electrode electrochemical cell at room temperature with graphite foil (20 x 10mm) as the counter electrode, Ni foam as the working electrode, and Ag/AgCl as reference electrode by using a CHI 660E model Electrochemical Workstation. The electrodeposition was carried out in aqueous solution containing $Ni(NO_3)_2$, Na_2MoO_2, and $Co(NO_3)_2$ with 1.2mM metal cations and varied Ni/Mo/Co molar ratios. The dry Ni foam was electrodeposited at constant current of $0.5mA/cm^2$ for 300 s at room temperature, right after soaking into the as-prepared solution for 900 s. The as-obtained coated Ni foam was dried in vacuum oven for another 24h. The mass of the Ni-Co-Mo active materials deposited on the Ni foam was carefully weighted before and after electrodeposition (after drying). Typical metal loading is ca. 0.1 mg.

3.2 Preparation of Ni-Mo-Co oxide nanoflakes

In a typical procedure, the as-prepared Ni-Mo-Co hydroxides substrate was further calcined at 400°C for 4 hours in Ar or N_2 gas with a temperature ramp rate of 2°C per minute. The mass of the Ni-Co-Mo active materials deposited on the Ni foam was carefully weighted before electrodeposition and after calcining. Typical metal loading is ca. 0.1 mg.

3.3 Materials characterization

The X-ray diffraction (XRD) patterns were obtained with a Bruker Phaser II. The X-ray photoelectron spectroscopy (XPS) spectra were detected by a Perkin-Elmer PHI 570 ESCA/SAM spectrometer. The morphology, surface structure and metal composition of the as-prepared samples were analyzed by field emission scanning electron microscopy (FE-SEM, JEOL JEM-7000F) and energy-dispersive X-ray spectroscopy (EDS, BRUKER QUANTAX EDS for SEM). Transmission electron microscopy (TEM) and selected area electron diffraction (SAED) patterns were obtained by a JEOL JEM-2010 microscope with LaB6 Filament gun.

3.4 Supercapacitor performance measurement

The single electrode supercapacitor measurements were carried out at room temperature using in a three-electrode cell system with as-prepared Ni foam substrate deposited with active materials, Pt foil and Hg/HgO as the working electrode, counter electrode, and reference electrode, respectively, using 30 c.c. of 1M aqueous KOH as the electrolyte. The cyclic voltammetry (CV), galvanostatic charge/discharge (GCD) and galvanostatic cycling performance (GCP) were tested by the electrochemical workstation (CHI 660E). The electrochemical impedance spectroscopy (EIS) measurements were obtained by using the GAMRY reference 300 electrochemical workstation.

3.5 Battery performance measurement

The half coin cells (CR 2032) for the LIB tests were assembled in an argon-filled glove box using as-prepared Ni foam as working electrode, lithium foil as counter and reference electrode, Celgard 2325 membrane as separator, and 1 M $LiPF_6$ in a solvent mixture of diethyl carbonate (DMC) and ethylene carbonate (EC) (1:1 by mass) as the electrolyte. The electrochemical impedance spectroscopy (EIS) measurements and cyclic voltammetry (CV) measurements were

tested on an electrochemical workstation (GAMRY reference 300). The cells were tested galvanostatically on a Battery Testing System at room temperature, in a voltage window ranging from 0.01 to 3.0 V (vs. Li/Li+) at various current densities.

CHAPTER 4. APPLICATION FOR SUPERCAPACITORS

4.1 Morphology and structural analysis

Ni-Mo-Co triple hydroxides (THs) ultrathin mesoporous nanoflakes (NFs) were deposited on Ni foam in the aqueous solution containing $Ni(NO_3)_2$, Na_2MoO_2, and $Co(NO_3)_2$ with total concentration of Ni^{2+}, Mo^{2+}, and Co^{2+} of 1.2 mM with varied Ni/Mo/Co molar ratios. The possible formation mechanism can be ascribed to the co-deposition of Ni_2^+, Co_2^+, and Mo^{6+} cations under alkaline condition. First, hydroxide ions (OH^-) are first produced at the surface of cathode by reduction reaction of NO^{3-} and H_2O, as shown in eqns (1) and (2):[79]

$$NO_3^- + 7H_2O + 8e^- \rightarrow NH_4^+ + 10OH^- \tag{1}$$

$$2H_2O + 2e^- \rightarrow H_2 + 2OH^- \tag{2}$$

Subsequently, the Ni-Co-Mo hydroxide was co-electrodeposited on a Ni foam surface according to eqn (3):[79]

$$x\,Ni^{2+} + y\,Co^{2+} + z\,Mo^{6+} + 2(x+y+3z)\,OH^- \rightarrow Ni_xCo_yMo_z(OH)_{2(x+y+3z)} \tag{3}$$
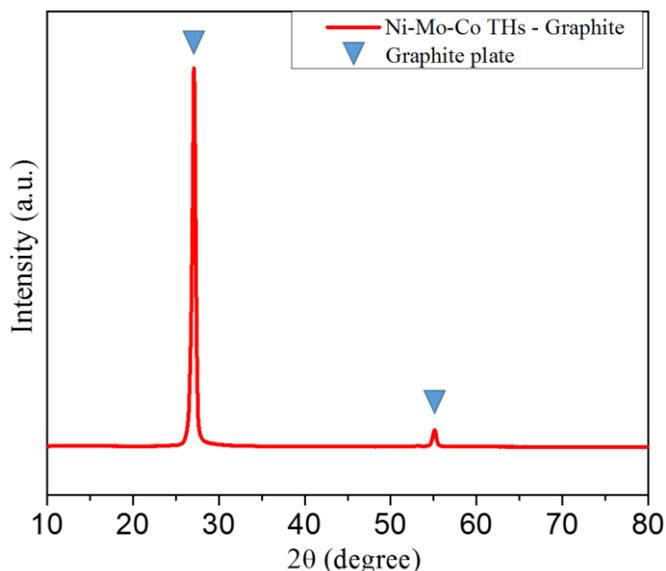
Fig. 4-1-1. XRD patterns of Ni-Mo-Co THs/ graphite obtained by electrodeposition in solution of Ni/Mo/Co (1/1/0.4).
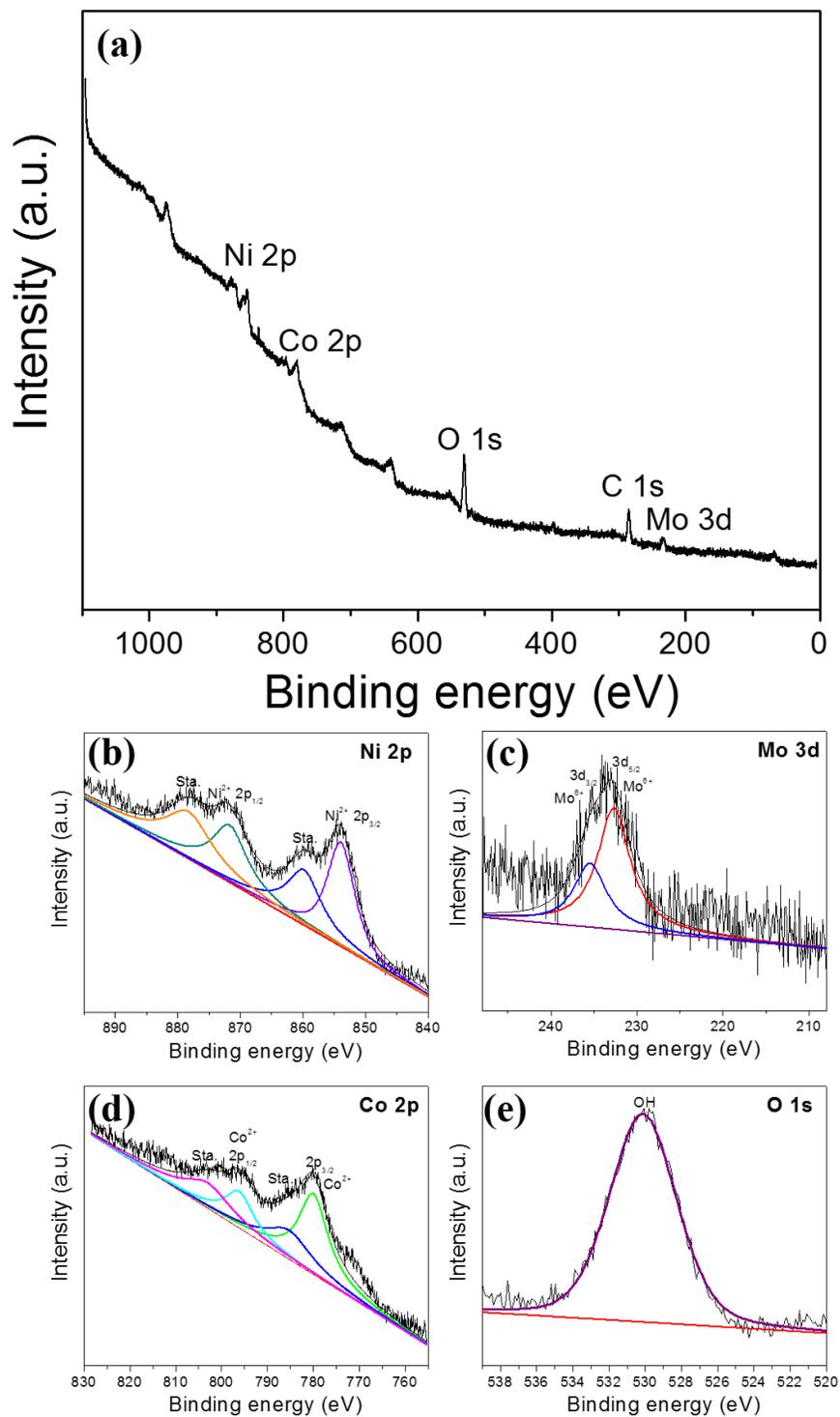
Fig. 4-1-2. XPS spectra of the Ni-Co-Mo hydroxide formed in Ni/Mo/Co (1/1/0.4) solution: (a) Survey scan, (b) Ni 2p spectrum, (c) Mo 3d spectrum, (d) Co 2p spectrum, (e) O 1s spectrum.

The XRD pattern (Fig. 4-1-1) shows only two peaks ($2\theta = 28^\circ$ and 55°) which can be attributed to the graphite substrate,[80] suggesting that the as-prepared Ni-Mo-Co THs is amorphous. The valence state information and surface composition of the as-prepared samples were detected by X-ray photoelectron spectroscopy (XPS), shown in Fig. 4-1-2. From the survey spectrum (Fig. 4-1-2 a), one can find the presence of Ni, Mo, Co, O as well as the small amount of Carbon. As shown in Fig. 4-1-2 b, the Ni emission spectrum was fitted with two strong spin-orbit doublet peaks and its shakeup satellites, the two major peaks with binding energies at 873.5 eV in $2p_{1/2}$ and 855.9 eV in $2p_{3/2}$ correspond to Ni^{2+} in Ni hydroxides.[81] The Mo 3d spectrum can be divided into two main peaks (Fig. 4-1-2 c). Two peaks with binding energies at 232.4 eV in $3d_{5/2}$ and 235.5 eV in $3d_{3/2}$, respectively, which are generally associated with Mo^{6+}.[82] Similar with Ni spectra, the Co high-resolution spectrum (Fig. 4-1-2 d) shows two peaks at 781.6 eV and 797.7 eV with its shakeup satellites peaks at 787.5 eV and 804 eV, which is a characteristic of Co^{2+} in Co hydroxides.[81, 83, 84] For the O 1s XPS spectrum (Fig. 1e), the peak at 531.1 eV can be attributed to metal-hydroxide bonds.[85] The XPS results illustrate that the element composition of the as-prepared sample contains Ni^{2+}, Mo^{6+} as well as Co^{2+}, indicating the Ni-Mo-Co ternary hydroxides were successfully synthesized.
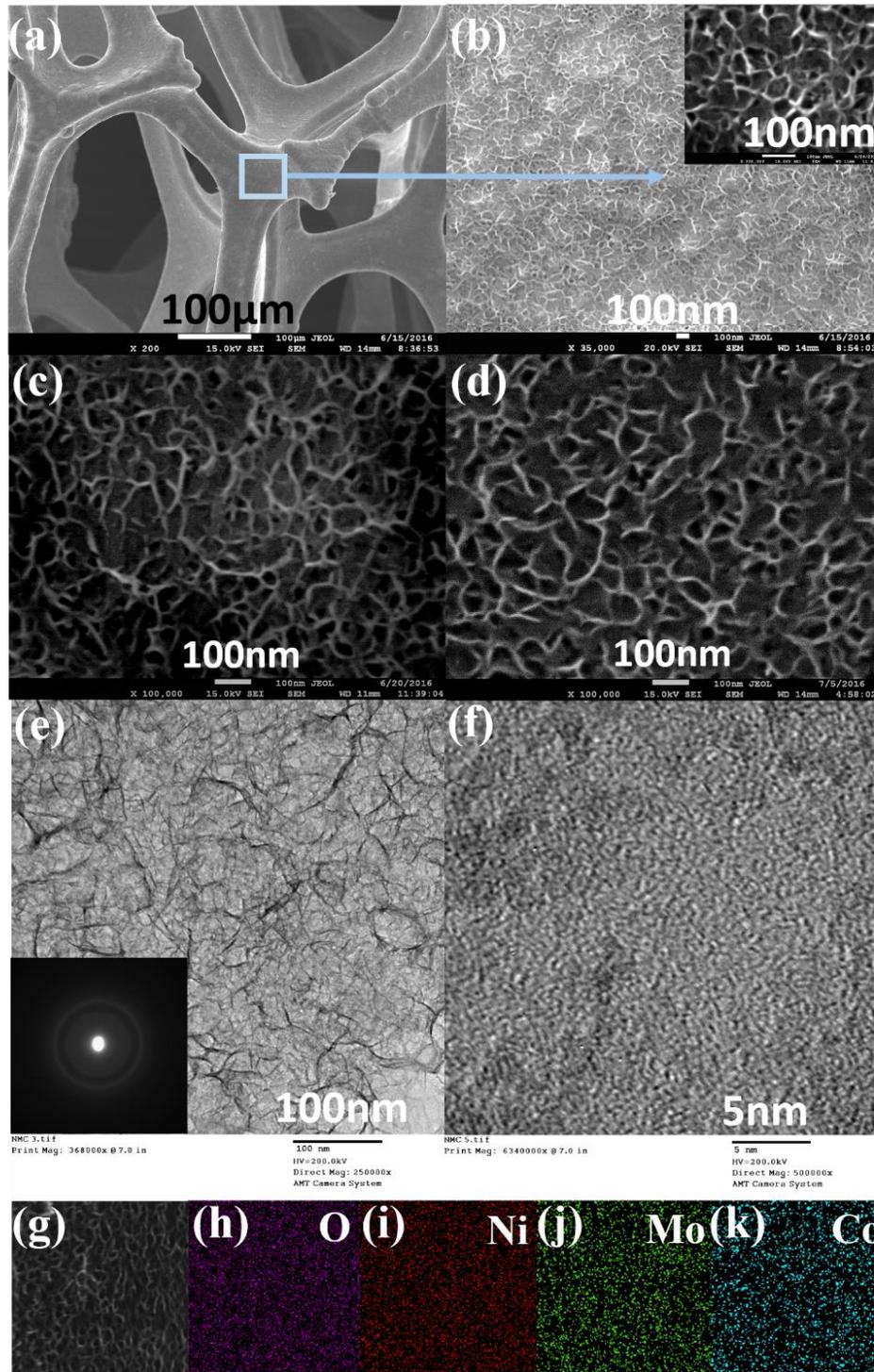
Fig. 4-1-3. Morphology of Ni-Co-Mo hydroxide formed in Ni/Mo/Co (1/1/0.4) solution: (a) low and (b) high magnification images Ni-Co-Mo NFs supported on Ni foam, the morphology and structure of Ni-Co-Mo NFs (c) before cycling and (d) after 5000 cycles test. (e) low and (f) high resolution TEM images of Ni-Co-Mo nanoflakes, the low-left inset in (e) represents he corresponding selected area diffraction pattern. (g-k) EDS elements mapping.

The SEM images (Fig. 4-1-3 a, b) show that Ni-Co-Mo THs, with the Ni/Mo/Co feeding ratio of 1/1/0.4, are deposited uniformly onto the macroscopic 3D skeleton of Ni foam. Fig. 4-1-3 b displays the SEM images recorded at higher magnification of the Ni foam surface marked in Fig. 4-1-3 a. The image shows the as-deposited ultrathin films consist of interconnected Ni-Mo-Co hydroxides platelets, forming mesoporous 3D nanostructure around 50nm in length, and 5 nm in thickness. These nanostructures tend to be vertically oriented on the surface of Ni foam, forming a nanoporous structure, with the pore size of about 50-100 nm. Different from pure Ni foam substrate, the highly rippled ultrathin nanoflakes 3D structure with abundant open space and a large surface to volume ratio which can provide more electroactive surface sites, resulting in the effective migration of the electrolyte within 3D structure and enhance mass/charge transfer at the electrode/electrolyte interface.[86] The morphology and structure of the as-deposited composites were further investigated by TEM. Fig. 4-1-3 e shows a panoramic view of the as-deposited Ni-Co-Mo THs nanoflakes. The interconnected mesoporous characteristic with a distinct light/dark contract suggested the existence of nanoflakes and the mesoporous structures with open space. Besides, the nanoflakes shows a rippled flack structure with a dimension around 50-100 nm, in accordance with the SEM results. These nanoflakes are quite transparent, indicating their ultrathin feature. Fig. 4-1-3 (g-k) presents the EDS-mapping images of the Ni-Mo-Co THs nanoflakes supported onto Ni foam. It clearly reveals that Mo, Ni, and Co elements are uniformly distributed on the whole test area, indicating the homogeneously deposition of the Ni-Mo-Co THs nanoflakes onto the skeleton of Ni foam.

The high resolution TEM image (Fig. 4-1-3 f) shows there is no detection of typical lattice fringes for Ni, Co, Mo of Ni-Mo-Co hydroxides composite, suggesting that the as-deposited Ni-Mo-Co THs nanoflakes are amorphous. This can be further supported by the selected-area

electron diffraction (SAED) pattern of the as-prepared nanoflakes (the inset of Fig. 4-1-3 e), which show a broad and diffused halo ring. As compared to crystalline metallic hydroxides, amorphous hydroxides exhibited enhanced electrochemical performance which may be due to the following aspects: 1. The long-range disorder and short-range ordered structure can improve the electronic conductivity of the electrode materials. 2. The easier access of amorphous structure for intercalation and deintercalation of charges; 3. Adequate defects on the amorphous materials favor the charge-transfer rate.[84] Also, the hierarchically structured electrode with mesoporous Ni-Co-Mo hydroxides formed on microporous Ni foam could benefit the ion/mass transfer while charging/ discharging.[7, 86]

4.2 Electrochemical performance of the supercapacitors (SCs)

The electrochemical properties were measured by CV and chronopotentiometry (CP) technique. Fig. 4-2-1 a presents the CV curves of Ni-Mo-Co nanoflakes electrode at various scan rates ranging from 1 mV s^{-1} to 50 mV s^{-1}. A pair of relatively symmetric, board redox peaks can be observed clearly in all the CV curves, which is characteristic of a pseudocapacitive behavior. The redox peaks were attributed corresponding to the Faradaic reactions of equation (1), (2), and (3), respectively.

$$Ni(OH)_2 + OH^- \leftrightarrow NiOOH + H_2O + e^- \tag{1}$$

$$Co(OH)_2 + OH^- \leftrightarrow CoOOH + H_2O + e^- \tag{2}$$

$$CoOOH + OH^- \leftrightarrow CoO_2 + H_2O + e^- \tag{3}$$
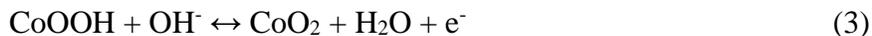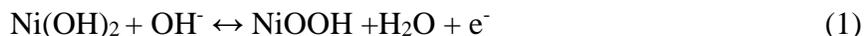
At the scan rate of 20 mV s^{-1}, the redox peak potentials are equal to 0.37 V (anodic peak) and 0.27 V (cathodic peak), respectively. Moreover, all of these CV curves exhibit similar shapes, except for the slight shift in the redox peak position with the increasing scan rates resulting from

concentration polarization,[87] indicating an appropriate electrochemical reversibility, high-rate performance as well as adequate electron conductivity of amorphous Ni-Mo-Co THs nanoflakes.[1] The galvanostatic charge-discharge (GCD) tests were performed within the potential window of –0.05 to 0.55 V (vs. Hg/HgO) at current densities varying from 2 to 50 A g^{-1} to evaluate the electrochemical capacitive performance (Fig. 4-2-1 b) using the chronopotentiometry (CP) technique. The nonlinear, highly symmetric shape, as well as obvious charge/discharge plateaus of the CP curves can also demonstrate the typical pseudocapacitance behavior.[4] Additionally, even at a high current density of 50 A g^{-1}. the charge/discharge curve still shows the nearly symmetric nature without an obvious IR drop (inset of Fig. 4-2-1 b). This suggests the amorphous Ni-Co-Mo hydroxide nanoflakes exhibit rapid *I-V* response characteristic and excellent reversible redox reaction, resulting in highly electrochemical reversibility.

Additionally, Fig. 4-2-1 c illustrates that there is a linear relationship between the square root of the scan rate and the corresponding current of the redox peaks, indicating that the electrochemical process is a diffusion-controlled process of hydroxyl ion.[1]
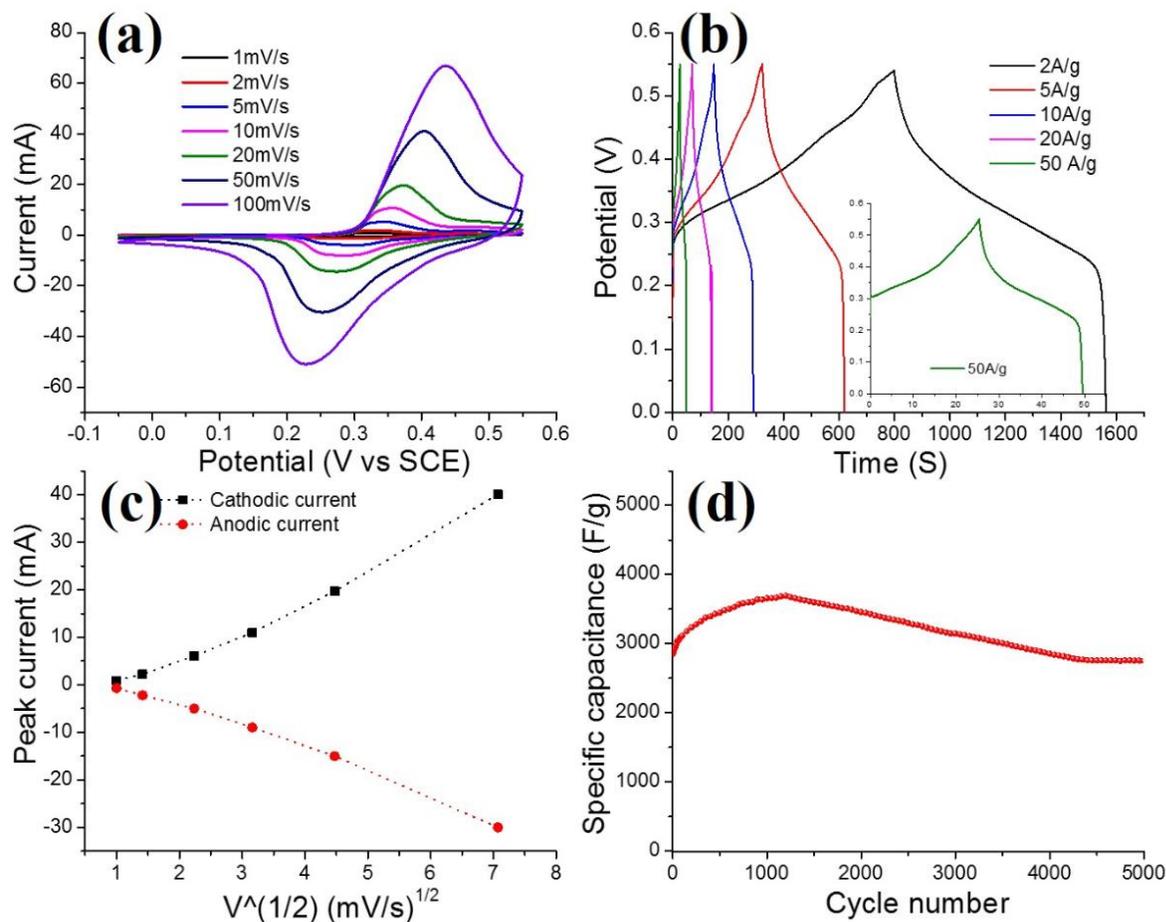
Fig. 4-2-1. (a) CV curves of the Ni-Co-Mo hydroxide supercapacitor (formed in Ni/Mo/Co (1/1/0.4) solution) at different scan rates from 1 to 100 mV s^{-1}, (b) galvanostatic charge/discharge (GCD) curves of the Ni-Co-Mo THs at different current densities from 2 to 50 A g^{-1}. (c) correlation between I_p and $V^{1/2}$ of the Ni-Mo-Co nanoflakes electrode, (d) Galvanostatic cycling performance at current density of 10 A g^{-1} for 5000 cycles.

The cycle stability is the most important factor for the practical application as an SC. Fig. 4-2-1 d shows the long-term performance of the Ni/Mo/Co (1/1/0.4) hydroxide nanoflakes electrode at a current density of 10 A g^{-1} Interestingly, specific capacitance of the Ni-Co-Mo hydroxide increased gradually during the first 1300 cycles, which can be attributed to activation of the electrode.[8, 88] Only 3.37 % of the specific capacitance was lost after 5000 charge/discharge cycles. and the morphology of Ni/Mo/Co (1/1/0.4) remains relatively stable (Fig. 4-1-3 c, d).

Thus, the remarkable cycling stability of this electrode can be attributed to the stable electrodeposited active materials on the Ni foam, as well as the resulting good structural stability.
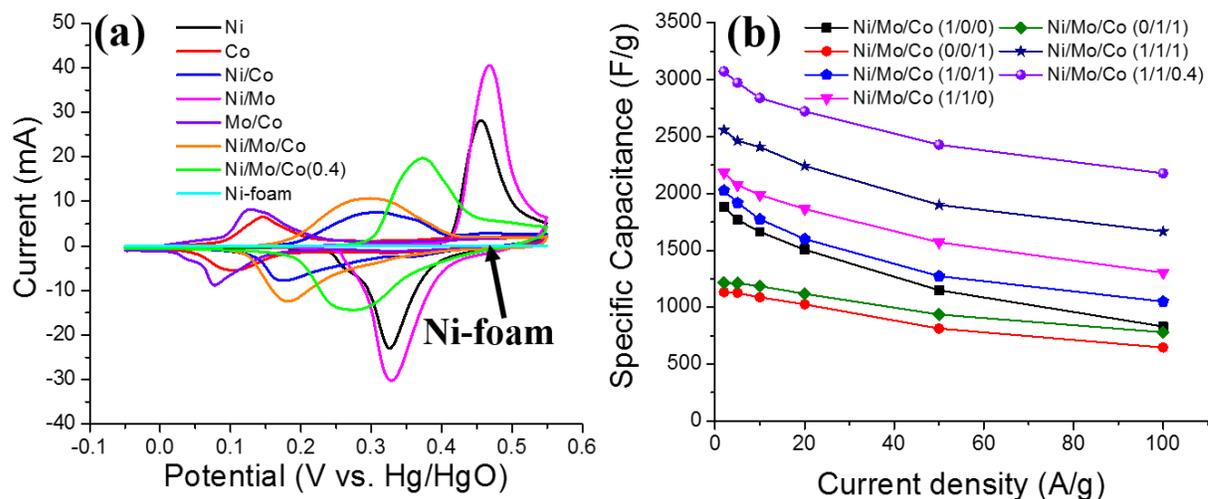
Fig. 4-2-2. Electrochemical properties of Ni-Mo-Co hydroxide supercapacitors formed in solution with different Ni/Co/Mo ratios: (a) CV curves at scanning rate of 20 mV/s, (b) evolution of specific capacitance with different current density.

Electrochemical performances of Ni-Mo-Co hydroxides with different Ni/Mo/Co ratios were investigated to reveal the effect of the Ni/Mo/Co composition on the properties of Ni-Mo-Co THs. Fig. 4-2-2 a presents the CV curves for the Ni-Mo-Co hydroxides within the potential window of -0.05 to 0.55 V (vs. Hg/HgO) at the scan rate of 20 mV s^{-1}. The redox peaks of Ni foam are significantly smaller than the as-deposited Ni-Mo-Co hydroxides electrodes, and the capacitance contributed from pure Ni-foam is negligible as shown in the Fig. 4-2-2 a. The Ni/Mo/Co (1/1/0) hydroxides show a pair of narrow redox peak in the potential range of 0.33 to 0.47 V. The anodic peak becomes stronger and broader with higher capacitance, and shifts to more negative potentials with increasing Co ratios.

The specific capacitance (C_s) as a function of current density of the Ni-Mo-Co THs nanoflakes were plotted in Fig. 4-2-2 b, calculated based on the discharge process in the CP measurement, using the following equation:[84]

$$C_s = I * \Delta t / m * \Delta V \qquad (4)$$

Where C_s represents the specific capacitance (F g^{-1}), I is the constant discharge current (A), Δt (s) is the duration of the discharge, m (g) is the mass of active material, and ΔV (V) is the voltage windows in the CP measurements. As expected, the specific capacitance of all samples decreases with the increasing of current density. This common pseudocapacitive behavior is due to lower rate of redox reactions at a higher current density as a result of a shorter time for ion diffusion.[4] The C_s of Ni/Mo/Co (1/0/1), Ni/Mo/Co (1/1/1), Ni/Mo/Co (0/0/1), and Ni/Mo/Co (0/1/1) are 2026.4 F g^{-1}, 2557.2 F g^{-1}, 1232.4 F g^{-1} and 1124.4 F g^{-1} , respectively, at the current density of 2 A g^{-1}. This suggests incorporation of Ni lead to a high electrochemical energy storage capacity. Similarly, incorporation of Mo resulting in a higher specific capacitance, as the C_s Mo containing samples of Ni/Mo/Co (0/1/1), Ni/Mo/Co (1/1/0), and Ni/Mo/Co (1/1/1) are 1124.4 F g^{-1}, 2026.4 F g^{-1}, and 2557.2 F g^{-1} (Fig. 4b) at the current density of 2 A g^{-1}, respectively. On the other hand, the C_s of Ni/Mo/Co (0/0/1), Ni/Mo/Co (1/0/0), and Ni/Mo/Co (1/0/1) are 1133.4 F g^{-1}, 1885.64 F g^{-1}, and 2026.4 F g^{-1} at the same current density, respectively, which are lower than the Mo-containing metal hydroxides. Among all samples, the Ni/Mo/Co (1/1/0.4) sample shows the highest specific capacitances of 3074 F g^{-1} at 2 A g^{-1}, and 2429 F g^{-1} at highest current of 50 A g^{-1} (ca. 80 % capacitance retention), indicating an excellent rate-performance and capacitance retention. On the other hand, capacitance retention of Ni/Mo/Co (1/1/0) and Ni/Mo/Co (1/1/1) are just ca. 72 % and ca. 74.3%, respectively. This excellent electrochemical performance can be attributed to the optimized amount of Co element, which may be attributed to the high electrochemical reversibility of Co-based hydroxides.[4] Moreover, the peak potential difference of Ni/Mo/Co (1/1/0.4) of ca. 100 mV is smaller than that of Ni/Mo (1/1) of ca. 140mV and Ni/Mo/Co (1/1/1) of ca. 110mV (Figure 4a). This phenomenon indicates a fairly high

electrochemical reversibility of Co.[4] Ni/Mo/Co (1/1/0.4) shows higher C_s (3074 F g^{-1} at 2 A g^{-1}) than Ni/Mo/Co (1/1/1) and all other samples, which maybe the result of optimal composition of triple metallic compositions. These results indicate that the tri-metallic hydroxide can further improve the specific capacitance as compared to bi-metallic hydroxide, which may attribute to the high electroactivity, stability and excellent reversibility with the addition of Co; [4, 5] fast electron transport, rapid ion diffusion, high electrical conductivity with Mo addition; [1] and remarkable electrochemical energy storage capacity resulting from Ni.[4, 86]
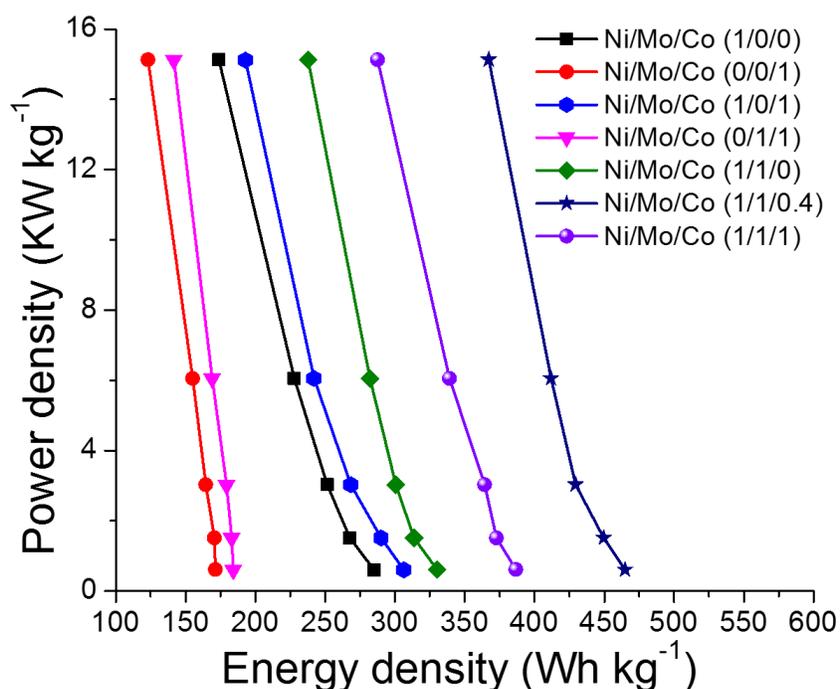
Fig. 4-2-3. Ragone chart of Ni-Mo-Co hydroxides formed in different solutions, obtained from the GCD tests.

Energy density (E), and power density (P) are both critical factors in evaluating the electrochemical performances of energy storage devices including supercapacitors. Fig. 4-2-3 presents the calculated gravimetric energy density and power density for the as-prepared hydroxide materials. It illustrates that the energy density of Ni/Mo/Co (1/1/0.4) is higher than

that of others at the same discharge in the current density. The Ni/Mo/Co (1/1/0.4) shows the highest energy density of 464.96 W h kg^{-1} among all materials at low current density, with a power density of 0.6 kW kg^{-1}; have an energy density of 367.39 W h kg^{-1}, which remains the highest among all materials at high current density with a great power density of 15.13 kW kg^{-1}, indicating a remarkable electrochemical performance as well.

CHAPTER 5. APPLICATION FOR LITHIUM-ION BATTERIES

5.1 The application for lithium-ion batteries

The idea of trimetallic compounds for energy storage can be used not only for supercapacitors (SCs) but also for rechargeable lithium-ion batteries (LIBs). In order to use in LIBs, the trimetallic hydroxides was converted to trimetallic oxides by calcination under an Ar atmosphere. The electrochemical performance of Ni-Mo-Co triple oxide (TOs) nanoflakes as binder-free anode materials for LIBs was studied. To get a better understanding on this part, a conventional Li-ion half coin cell with 1 M $LiPF_6$ in a solvent mixture of diethyl carbonate (DMC) and ethylene carbonate (EC) (1:1 by mass) as the electrolyte has been used.

5.2 Electrochemical Performance of Ni-Mo-Co TOs

Cyclic voltammetry (CV) test

To study the Li-ion insertion and extraction reaction of these materials during discharging and charging, the CV measurement was tested in a potential range of 0.01 to 3 V (vs. Li/Li^+) with the scan rate of 0.5 mV s^{-1}. The first three cycles of CV curves of Ni-Mo-Co TOs are displayed in Fig. 5-2-1. As shown in Fig. 5-2-1 a, the profiles of CV curves from the 2nd and 3rd cycle are similar, whereas a different curve has been showed in the 1st cycle from those of the subsequent cycles. In the 1st cathodic sweep, a sharp and strong cathodic peak located at ca. 0.34 V could be ascribed to the lithium insertion reaction. This strong peak maybe attributed to the formation of a solid-electrolyte interphase (SEI) layer at the interface of electrode and electrolyte[89, 90] as a result of reduction of Ni^{2+}, Mo^{6+}, and Co^{2+} to form Ni, Mo, Co, as well as Li_2O (from the decomposition of Ni-Co-Mo TOs), which are shown in equations (1) and (2). The main reduction peak shifts to positive potential and decrease in the peak intensity, located at ca. 1.02 V in the subsequent cycles, resulting from the pulverization of the Ni-Mo-Co triple oxides

since the irreversible Li-ion loss during the SEI formation.[91] In addition, this loss may be also associated with the formation of the SEI layer, resulting from the electrolyte decomposition or side reactions. The following anodic sweep is characterized by two oxidation peaks in the first CV curve located at ca. 1.55 and ca. 2.25 V respectively, which could be assigned to the oxidation of Ni to NiO, Mo to MoO$_3$, and Co to CoO, as shown in equations (3), (4), and (5), respectively.[89, 90, 92, 93]

$$10 \, Li \rightarrow 10 \, Li^+ + 10 \, e^- \tag{1}$$

$$NiCoMoO_5 + 10 \, Li^+ \rightarrow Ni + Mo + Co + 5 \, Li_2O \tag{2}$$

$$Ni + Li_2O \rightarrow NiO + 2 \, Li^+ + 2 \, e^- \tag{3}$$

$$Mo + 3 \, Li_2O \rightarrow MoO_3 + 6 \, Li^+ + 6 \, e^- \tag{4}$$

$$Co + Li_2O \rightarrow CoO + 2 \, Li^+ + 2 \, e^- \tag{5}$$
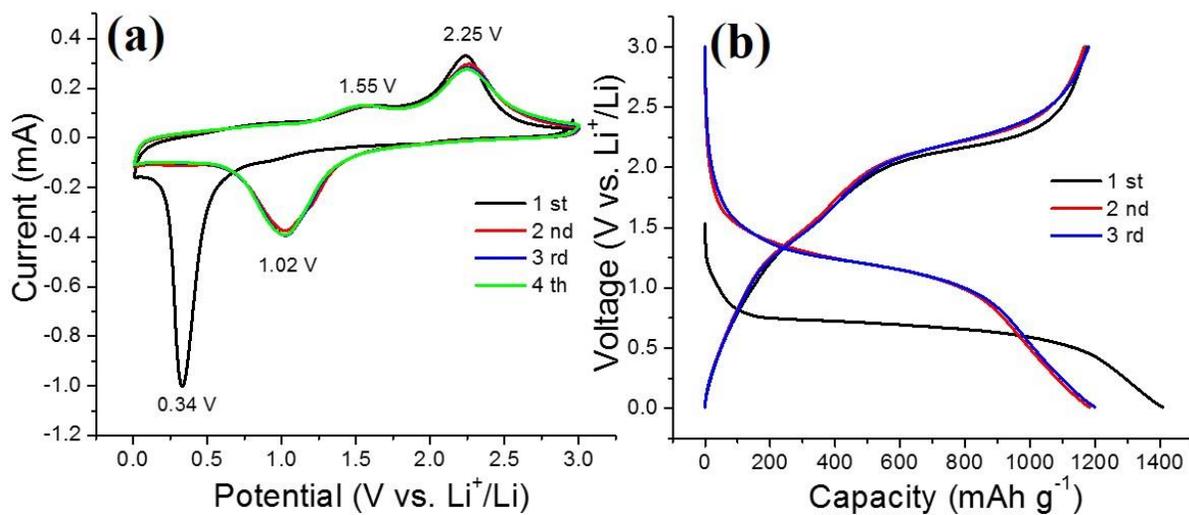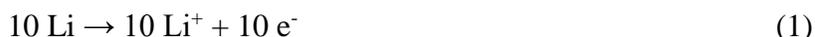
Fig. 5-2-1. (a) CV curves of the Ni-Mo-Co TOs nanoflakes at a scan rate of 0.5 mV s^{-1}. (b) The first three cycles charge-discharge voltage profiles of Ni-Mo-Co TOs nanoflakes.

It is noteworthy that there is no significant shift of CV shapes since the 2nd cycle, indicating a good reproducibility and remarkable electrochemical reversibility of the redox reaction.

Charge-discharge reaction mechanism

The Li-storage properties of Ni-Mo-Co TOs nanoflakes were investigated by galvanostatic charge-discharge in the voltage window 0.001 - 3.0 V at a current density of 0.2 A g^{-1}. The typical charge-discharge voltage profiles of Ni-Mo-Co TOs nanoflakes electrode for the first three cycles at a current density of are presented in Figure 5-2-1 b. It illustrates that for the first cycle, a small discharge voltage plateau can be observed at between 0.467 V to 0.8 V followed by continuous decrease in voltage up to the cut-off voltage, which is 0.01 V. Next charging to 3 V, two smooth voltage plateau can be seen till ca. 1.55 V and 2.25 V which is followed by upward sloping voltage plateau up to ca. 1.8 V and 2.5 V respectively, then a gradual rise to 3.0 V. The first and all the subsequent discharge curves shows one plateau between 0.467 to 0.8 V, and 0.9 to 1.5 V, respectively, which corresponds well with the CV results. In addition, the plateau of the first discharge curve is lower than others, resulting from the irreversible reaction between Ni-Mo-Co oxides and Li+ as equation (2) as well as the SEI formation. It is worth noting that the first cycle discharge and charge capacities are 1408.06 mA h g^{-1} and 1170.28 mA h g^{-1}, respectively. The lower irreversible initial coulombic efficiency (83.1%) can be due to small amount SEI layer formation since the capacity below 0.3V is only about 200mA h/ g^{-1} in the 1st cycle. In the subsequent charging cycles, the two voltage plateaus are located at ca. 1.55 V and ca. 2.25 V, corresponding to the extraction reaction of Li$^+$ to form lithiated NiO and CoO, and MoO$_3$, respectively, which is similar with the CV peaks. Moreover, the coulombic efficiency increases from 93.4 % in the initial cycle to 99 % in the second cycle, and then remains around 99 % during the following cycles, indicates the remarkable reversibility of Ni-Mo-Co TOs materials for an anode electrode.

5.3 Electrochemical evaluation of Ni-Mo-Co TOs

To get a better understanding on the electrochemical behavior of Ni-Mo-Co TOs as an anode materials in LIBs. A series of electrochemical measurements have been tested, including rate performance measurement as well as the cycling test, as shown in Figure 5-3-1.

Rate performance

The rate capability of LIB anodes is highly crucial, to evaluate the rate performance, the Ni-Mo-Co TOs were cycled at various current densities from 0.2 A g^{-1} to 5 A g^{-1} and returned to 0.2 A g^{-1}, for 10 cycles at each current density (Figure 5-3-1 a). The 1st cycle irreversible capacity losses were attributed to irreversible Li-insertion, decomposition of the electrolyte, and the formation of SEI layer.[90, 92] The half coin cell shows the capacity raised occurred during the first ten cycles at 0.2 A g^{-1}, resulting from the full activation of Ni-Mo-Co TOs electrode.[94] The reversible capacity of Ni-Mo-Co TOs was as high as 1160.0 mA h g^{-1} after ten cycles at 0.2 A g^{-1}. The cell shows good rate capability with perfect maintained average discharge capacity of 1132.31 mA h g^{-1}, 1141.45 mA h g^{-1}, 1109.87 mA h g^{-1}, 1045.58 mA h g^{-1}, 945.35 mA h g^{-1}, 844.73 mA h g^{-1}, 756.9 mA h g^{-1}, when the current density increased stepwise to 0.2 A g^{-1}, 0.5 A g^{-1}, 1 A g^{-1}, 2 A g^{-1}, 3 A g^{-1}, 4 A g^{-1}, 5 A g^{-1} (1 C = 1 A g^{-1}), respectively. Clearly, the decrease of discharge capacity with an increase in charge-discharge current density was very slow, implying its good rate performance. Besides, the coulombic efficiency increases from 83.1 % in the 1st cycle to 98.8 % at the 2nd cycle, and remain above 96 % in the following cycles. It is worth considering that the capacity reverted to 1240.13 mA h g^{-1} in average, when the current density returned to 0.2 A g^{-1}, indicating the good structural stability and remarkable rate performance of as-prepared Ni-Mo-Co TOs nanoflakes.
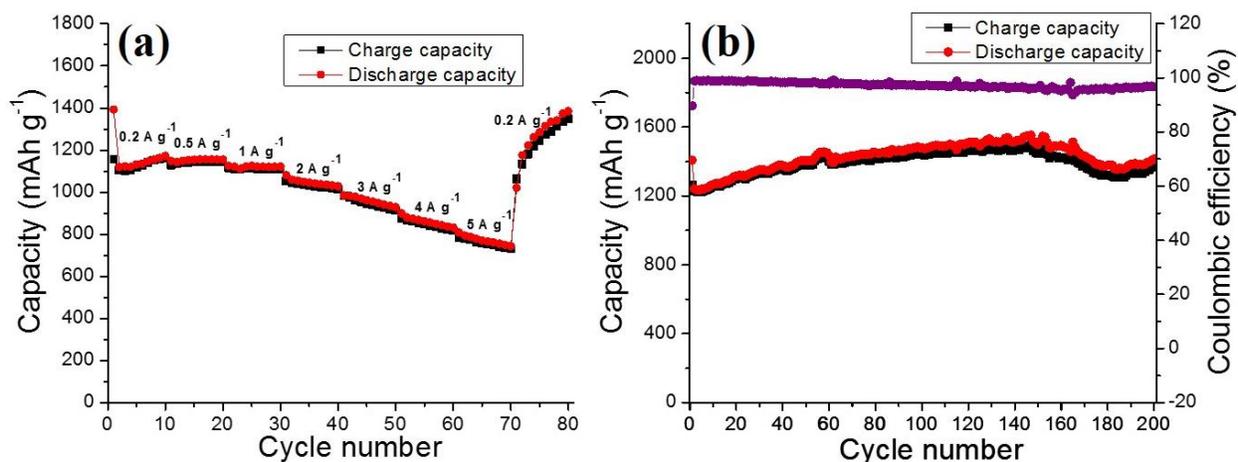
Fig. 5-3-1. (a) The specific capacity of the Ni-Mo-Co TOs nanoflakes at various current densities. (b) The specific capacity and coulombic efficiency for 200 cycles charge-discharge at 1 A g^{-1} for Ni-Mo-Co TOs nanoflakes.

Galvanostatic Cycling

The galvanostatic cycling measurement were tested at a current density of 1 A g^{-1} for 200 cycles to further understand the cyclability of Ni-Mo-Co TOs anode materials. As shown in Figure 5-3-1 b, it presents the cycling performance and coulombic efficiency of the Ni-Mo-Co TOs electrode. It shows significantly improved capacities through the charging-discharging until 150 cycles. After 200 cycles, the discharge capacities were stable at 1415.3 mA h g^{-1}, and no capacity decay was observed. After the 1st cycle, the coulombic efficiency rapidly increased to ca. 100 % in the subsequence cycles, and was maintained at above 98% for all 200 cycles. These results demonstrate the high-performance and excellent cycle stability of Ni-Mo-Co TOs as an anode materials in LIBs.

CHAPTER 6. CONCLUSION

In summary, amorphous Ni-Mo-Co triple hydroxides nanoflakes as electrodes for SCs were synthesized via a facile template-free, and scalable electrodeposition method. Besides, Ni-Mo-Co tri-metallic oxides as anode materials for LIBs were prepared via further calcination of triple metal hydroxides samples. The ultrathin mesoporous Ni-Mo-Co THs/TOs nanoflakes on Ni-foam were evaluated as a binder-free electrode for SCs and LIBs, respectively. The large open spaces between the interconnected mesoporous nanoflakes provide more electroactive surface sites and a facile electron transmission path, resulting in high specific capacitance and capacity (3074 F g^{-1} at 2 A g^{-1}, and 2429 F g^{-1} at highest current of 50 A g^{-1} in SCs; 1132.31 mA h g^{-1} at 0.2 A g^{-1} and 756.9 mA h g^{-1} at 5 A g^{-1} in LIBs), outstanding rate performance (80 % capacitance retention from 2 A g^{-1} to 50 A g^{-1} in SCs and 66.84 % capacity retention from 0.2 A g^{-1} to 5 A g^{-1} in LIBs), and remarkable cyclability (96.63 % of capacitance retention after 5000 cycles in SCs at current density of 10 A g^{-1};, and no capacity decay was observed after 200 cycles in LIBs at current density of 1 A g^{-1}).

The excellent electrochemical performance of high specific capacitance/capacity, long cyclability as well as good rate performance for Ni-Mo-Co triple hydroxides nanoflakes with desirable composition for SCs could be attributed to: (1) the mesoporous hierarchical architectures of Ni-Mo-Co hydroxides nanoflakes[95] and 3D structure with abundant open spaces affording a continuous network as well as extra active sites for the redox reaction with charge/discharge, increasing the contact area between the electrode and electrolyte.[18] (2) the ultrathin nanoflakes significantly shorten the ion (OH$^-$ in SCs or Li$^+$ in LIBs) diffusion length, increasing the rate performance. (3) the amorphous nature of as-obtained triple metallic hydroxide with more defects, long-range disorder, as well as short-range order which help to

obtain the excellent electrochemical performance.[84] (4) the active materials directly grown on Ni-foam substrates provide effective electron transport pathways between the Ni-foam and active materials, besides the binder-free electrodes system that can avoid the insufficient contact between the electrolyte and electroactive sites, promote the electrolyte penetration into the active material, resulting in the fast transportation of electrons and high rate capability.[86, 96]

In addition, the Ni-Mo-Co oxides binder-free electrodes for LIBs exhibited excellent rate performance and cyclability. The preliminary results for LIBs application shows that the as-prepared materials are promising high-capacity anode materials for LIBs to substitute conventional carbon-based anode materials with theoretical capacity of 372 mA h g^{-1} only.

Overall, a bifunctional electrode material was developed for high performance energy storage systems, as well as a facile and scalable fabrication method to design other ternary metal hydroxides/oxides nanostructured electrodes for energy storage materials research and development.

REFERENCES

[1] Xiao K, Xia L, Liu G, Wang S, Ding L-X, Wang H. Honeycomb-like $NiMoO_4$ ultrathin nanosheet arrays for high-performance electrochemical energy storage. Journal of Materials Chemistry A. 2015;3:6128-35.

[2] Miller JR, Simon P. Electrochemical Capacitors for Energy Management. Science. 2008;321:651-2.

[3] Liu C, Li F, Ma L-P, Cheng H-M. Advanced Materials for Energy Storage. Advanced Materials. 2010;22:E28-E62.

[4] Hu C-C, Chen J-C, Chang K-H. Cathodic deposition of $Ni(OH)_2$ and $Co(OH)_2$ for asymmetric supercapacitors: Importance of the electrochemical reversibility of redox couples. Journal of Power Sources. 2013;221:128-33.

[5] Xing J, Wu S, Ng KYS. Electrodeposition of ultrathin nickel-cobalt double hydroxide nanosheets on nickel foam as high-performance supercapacitor electrodes. RSC Advances. 2015;5:88780-6.

[6] Zhang G, Lou XW. General Solution Growth of Mesoporous $NiCo_2O_4$ Nanosheets on Various Conductive Substrates as High-Performance Electrodes for Supercapacitors. Advanced Materials. 2013;25:976-9.

[7] Yin Z, Zhang S, Chen Y, Gao P, Zhu C, Yang P, et al. Hierarchical nanosheet-based $NiMoO_4$ nanotubes: synthesis and high supercapacitor performance. Journal of Materials Chemistry A. 2015;3:739-45.

[8] Yuan C, Li J, Hou L, Zhang X, Shen L, Lou XW. Ultrathin Mesoporous NiCo2O4 Nanosheets Supported on Ni Foam as Advanced Electrodes for Supercapacitors. Advanced Functional Materials. 2012;22:4592-7.

[9] Yu X, Lu B, Xu Z. Super Long-Life Supercapacitors Based on the Construction of Nanohoneycomb-Like Strongly Coupled CoMoO4–3D Graphene Hybrid Electrodes. Advanced Materials. 2014;26:1044-51.

[10] Guo D, Zhang H, Yu X, Zhang M, Zhang P, Li Q, et al. Facile synthesis and excellent electrochemical properties of CoMoO4 nanoplate arrays as supercapacitors. Journal of Materials Chemistry A. 2013;1:7247-54.

[11] Mai L-Q, Yang F, Zhao Y-L, Xu X, Xu L, Luo Y-Z. Hierarchical MnMoO4/CoMoO4 heterostructured nanowires with enhanced supercapacitor performance. Nature Communications. 2011;2:381.

[12] Mondal AK, Su D, Chen S, Ung A, Kim H-S, Wang G. Mesoporous MnCo2O4 with a Flake-Like Structure as Advanced Electrode Materials for Lithium-Ion Batteries and Supercapacitors. Chemistry – A European Journal. 2015;21:1526-32.

[13] Padmanathan N, Selladurai S. Mesoporous MnCo2O4 spinel oxide nanostructure synthesized by solvothermal technique for supercapacitor. Ionics. 2014;20:479-87.

[14] Li M, Cheng JP, Wang J, Liu F, Zhang XB. The growth of nickel-manganese and cobalt-manganese layered double hydroxides on reduced graphene oxide for supercapacitor. Electrochimica Acta. 2016;206:108-15.

[15] Zhao J, Chen J, Xu S, Shao M, Yan D, Wei M, et al. CoMn-layered double hydroxide nanowalls supported on carbon fibers for high-performance flexible energy storage devices. Journal of Materials Chemistry A. 2013;1:8836-43.

[16] Guo XL, Liu XY, Hao XD, Zhu SJ, Dong F, Wen ZQ, et al. Nickel-Manganese Layered Double Hydroxide Nanosheets Supported on Nickel Foam for High-performance Supercapacitor Electrode Materials. Electrochimica Acta. 2016;194:179-86.

[17] Ma K, Cheng JP, Liu F, Zhang X. Co-Fe layered double hydroxides nanosheets vertically grown on carbon fiber cloth for electrochemical capacitors. Journal of Alloys and Compounds. 2016;679:277-84.

[18] Zhang Y, Li L, Su H, Huang W, Dong X. Binary metal oxide: advanced energy storage materials in supercapacitors. Journal of Materials Chemistry A. 2015;3:43-59.

[19] Wang A-L, Xu H, Li G-R. NiCoFe Layered Triple Hydroxides with Porous Structures as High-Performance Electrocatalysts for Overall Water Splitting. ACS Energy Letters. 2016;1:445-53.

[20] Chen-Wiegart Y-cK, Liu Z, Faber KT, Barnett SA, Wang J. 3D analysis of a LiCoO2–Li(Ni1/3Mn1/3Co1/3)O2 Li-ion battery positive electrode using x-ray nano-tomography. Electrochemistry Communications. 2013;28:127-30.

[21] Ecker M, Nieto N, Käbitz S, Schmalstieg J, Blanke H, Warnecke A, et al. Calendar and cycle life study of Li(NiMnCo)O2-based 18650 lithium-ion batteries. Journal of Power Sources. 2014;248:839-51.

[22] Xiao H, Yao S, Liu H, Qu F, Zhang X, Wu X. NiO nanosheet assembles for supercapacitor electrode materials. Progress in Natural Science: Materials International. 2016;26:271-5.

[23] Rakhi RB, Chen W, Hedhili MN, Cha D, Alshareef HN. Enhanced Rate Performance of Mesoporous Co3O4 Nanosheet Supercapacitor Electrodes by Hydrous RuO2 Nanoparticle Decoration. ACS Applied Materials & Interfaces. 2014;6:4196-206.

[24] Huang Y, Li Y, Hu Z, Wei G, Guo J, Liu J. A carbon modified MnO2 nanosheet array as a stable high-capacitance supercapacitor electrode. Journal of Materials Chemistry A. 2013;1:9809-13.

[25] Mirvakili SM, Mirvakili MN, Englezos P, Madden JDW, Hunter IW. High-Performance Supercapacitors from Niobium Nanowire Yarns. ACS Applied Materials & Interfaces. 2015;7:13882-8.

[26] Dong X, Guo Z, Song Y, Hou M, Wang J, Wang Y, et al. Flexible and Wire-Shaped Micro-Supercapacitor Based on Ni(OH)2-Nanowire and Ordered Mesoporous Carbon Electrodes. Advanced Functional Materials. 2014;24:3405-12.

[27] Lv J, Yang X, Zhou H, Kang L, Lei Z, Liu Z-H. MnO2-wrapped hollow graphitized carbon nanosphere electrode for supercapacitor. Materials Research Bulletin. 2016;73:429-36.

[28] Javed MS, Dai S, Wang M, Guo D, Chen L, Wang X, et al. High performance solid state flexible supercapacitor based on molybdenum sulfide hierarchical nanospheres. Journal of Power Sources. 2015;285:63-9.

[29] Zhang D, Zhang X, Chen Y, Wang C, Ma Y, Dong H, et al. Supercapacitor electrodes with especially high rate capability and cyclability based on a novel Pt nanosphere and cysteine-generated graphene. Physical Chemistry Chemical Physics. 2012;14:10899-903.

[30] Anandan S, Chen C-Y, Wu JJ. Sonochemical synthesis and characterization of turbostratic MnNi(OH)2 layered double hydroxide nanoparticles for supercapacitor applications. RSC Advances. 2014;4:55519-23.

[31] Halper MS, Ellenbogen JC. Supercapacitors: A brief overview. The MITRE Corporation, McLean, Virginia, USA. 2006:1-34.

[32] Srinivasan S. Electrode/electrolyte interfaces: Structure and kinetics of charge transfer. Fuel Cells: Springer; 2006. p. 27-92.

[33] Kötz R, Carlen M. Principles and applications of electrochemical capacitors. Electrochimica acta. 2000;45:2483-98.

[34] Frackowiak E, Beguin F. Carbon materials for the electrochemical storage of energy in capacitors. Carbon. 2001;39:937-50.

[35] Sparnaay MJ. The electrical double layer: Pergamon; 1972.

[36] Conway BE. Transition from "supercapacitor" to "battery" behavior in electrochemical energy storage. Journal of the Electrochemical Society. 1991;138:1539-48.

[37] Conway B. Electrochemical Supercapacitors-Scientific Fundamentals and Technological Applications Plenum Press. New York. 1999.

[38] Namisnyk AM. A survey of electrochemical supercapacitor technology: University of Technology, Sydney; 2003.

[39] Zhang LL, Zhao XS. Carbon-based materials as supercapacitor electrodes. Chemical Society Reviews. 2009;38:2520-31.

[40] Pandolfo A, Hollenkamp A. Carbon properties and their role in supercapacitors. Journal of power sources. 2006;157:11-27.

[41] Fischer U, Saliger R, Bock V, Petricevic R, Fricke J. Carbon aerogels as electrode material in supercapacitors. Journal of Porous Materials. 1997;4:281-5.

[42] Presser V, Heon M, Gogotsi Y. Carbide‐Derived Carbons‐From Porous Networks to Nanotubes and Graphene. Advanced Functional Materials. 2011;21:810-33.

[43] Yoo JJ, Balakrishnan K, Huang J, Meunier V, Sumpter BG, Srivastava A, et al. Ultrathin planar graphene supercapacitors. Nano letters. 2011;11:1423-7.

[44] Palaniselvam T, Baek J-B. Graphene based 2D-materials for supercapacitors. 2D Materials. 2015;2:032002.

[45] Li X, Rong J, Wei B. Electrochemical behavior of single-walled carbon nanotube supercapacitors under compressive stress. ACS nano. 2010;4:6039-49.

[46] Simon P, Gogotsi Y. Materials for electrochemical capacitors. Nat Mater. 2008;7:845-54.

[47] Lukatskaya MR, Mashtalir O, Ren CE, Dall'Agnese Y, Rozier P, Taberna PL, et al. Cation Intercalation and High Volumetric Capacitance of Two-Dimensional Titanium Carbide. Science. 2013;341:1502-5.

[48] Wang G, Zhang L, Zhang J. A review of electrode materials for electrochemical supercapacitors. Chemical Society Reviews. 2012;41:797-828.

[49] Yan J, Fan Z, Sun W, Ning G, Wei T, Zhang Q, et al. Advanced Asymmetric Supercapacitors Based on Ni(OH)2/Graphene and Porous Graphene Electrodes with High Energy Density. Advanced Functional Materials. 2012;22:2632-41.

[50] Meng X, Deng D. Bio-inspired synthesis of [small alpha]-Ni(OH)2 nanobristles on various substrates and their applications. Journal of Materials Chemistry A. 2016;4:6919-25.

[51] Cao L, Xu F, Liang YY, Li HL. Preparation of the Novel Nanocomposite Co(OH)2/ Ultra-Stable Y Zeolite and Its Application as a Supercapacitor with High Energy Density. Advanced Materials. 2004;16:1853-7.

[52] Deng W, Lan W, Sun Y, Su Q, Xie E. Porous CoO nanostructures grown on three-dimension graphene foams for supercapacitors electrodes. Applied Surface Science. 2014;305:433-8.

[53] Zhou C, Zhang Y, Li Y, Liu J. Construction of High-Capacitance 3D CoO@Polypyrrole Nanowire Array Electrode for Aqueous Asymmetric Supercapacitor. Nano Letters. 2013;13:2078-85.

[54] Hu C-C, Chang K-H, Lin M-C, Wu Y-T. Design and Tailoring of the Nanotubular Arrayed Architecture of Hydrous RuO2 for Next Generation Supercapacitors. Nano Letters. 2006;6:2690-5.

[55] Du X, Wang C, Chen M, Jiao Y, Wang J. Electrochemical Performances of Nanoparticle Fe3O4/Activated Carbon Supercapacitor Using KOH Electrolyte Solution. The Journal of Physical Chemistry C. 2009;113:2643-6.

[56] Snook GA, Kao P, Best AS. Conducting-polymer-based supercapacitor devices and electrodes. Journal of Power Sources. 2011;196:1-12.

[57] Volfkovich YM, Mikhailin A, Bograchev D, Sosenkin V, Bagotsky V. Studies of supercapacitor carbon electrodes with high pseudocapacitance: INTECH Open Access Publisher; 2012.

[58] Szubzda B, Szmaja A, Ozimek M, Mazurkiewicz S. Polymer membranes as separators for supercapacitors. Applied Physics A. 2014;117:1801-9.

[59] Karabelli D, Lepretre J-C, Alloin F, Sanchez J-Y. Poly (vinylidene fluoride)-based macroporous separators for supercapacitors. Electrochimica Acta. 2011;57:98-103.

[60] Nanda J, Ruther RE, Delnick FM, Sun C-N. Electrolytes for supercapacitors. Google Patents; 2016.

[61] Lee HY, Goodenough JB. Supercapacitor Behavior with KCl Electrolyte. Journal of Solid State Chemistry. 1999;144:220-3.

[62] Nam K-W, Lee C-W, Yang X-Q, Cho BW, Yoon W-S, Kim K-B. Electrodeposited manganese oxides on three-dimensional carbon nanotube substrate: Supercapacitive behaviour in aqueous and organic electrolytes. Journal of Power Sources. 2009;188:323-31.

[63] Jiang J, Kucernak A. Electrochemical supercapacitor material based on manganese oxide: preparation and characterization. Electrochimica Acta. 2002;47:2381-6.

[64] Etacheri V, Marom R, Elazari R, Salitra G, Aurbach D. Challenges in the development of advanced Li-ion batteries: a review. Energy & Environmental Science. 2011;4:3243-62.

[65] Sasaki T, Ukyo Y, Novák P. Memory effect in a lithium-ion battery. Nature materials. 2013;12:569-75.

[66] Leiva L. Memory Effect Now Also Found in Lithium-Ion Batteries. Luettavissa: http://phys org/news/2013-04-memory-effect-lithium-ion-batteries html Luettu. 2013;22:2016.

[67] Linden D, Reddy TB. Handbook of Batteries. 3rd. McGraw-Hill; 2002.

[68] Gabano J-P. Lithium batteries. London and New York, Academic Press, 1983, 467 p. 1983;1.

[69] Brandt K. Historical development of secondary lithium batteries. Solid State Ionics. 1994;69:173-83.

[70] Mohanty D, Sefat AS, Kalnaus S, Li J, Meisner RA, Payzant EA, et al. Investigating phase transformation in the Li1.2Co0.1Mn0.55Ni0.15O2 lithium-ion battery cathode during high-voltage hold (4.5 V) via magnetic, X-ray diffraction and electron microscopy studies. Journal of Materials Chemistry A. 2013;1:6249-61.

[71] Dolotko O, Senyshyn A, Mühlbauer MJ, Nikolowski K, Ehrenberg H. Understanding structural changes in NMC Li-ion cells by in situ neutron diffraction. Journal of Power Sources. 2014;255:197-203.

[72] Hu L-H, Wu F-Y, Lin C-T, Khlobystov AN, Li L-J. Graphene-modified LiFePO4 cathode for lithium ion battery beyond theoretical capacity. Nature communications. 2013;4:1687.

[73] Li Y-D, Zhao S-X, Nan C-W, Li B-H. Electrochemical performance of SiO2-coated LiFePO4 cathode materials for lithium ion battery. Journal of Alloys and Compounds. 2011;509:957-60.

[74] Meduri P, Pendyala C, Kumar V, Sumanasekera GU, Sunkara MK. Hybrid Tin Oxide Nanowires as Stable and High Capacity Anodes for Li-Ion Batteries. Nano Letters. 2009;9:612-6.

[75] Wu HB, Chen JS, Hng HH, Wen Lou X. Nanostructured metal oxide-based materials as advanced anodes for lithium-ion batteries. Nanoscale. 2012;4:2526-42.

[76] Reddy T. Linden D. Linden's handbook of batteries. New York: McGraw-Hill; 2011.

[77] Tarascon JM, Armand M. Issues and challenges facing rechargeable lithium batteries. Nature. 2001;414:359-67.

[78] Abruña HD, Kiya Y, Henderson JC. Batteries and electrochemical capacitors. Phys Today. 2008;61:43-7.

[79] Sasaki Y, Yamashita T. Effect of electrolytic conditions on the deposition of nickel hydroxide. Thin Solid Films. 1998;334:117-9.

[80] Yu M, Liu P-R, Sun Y-J, Liu J-H, An J-W, Li S-M. Fabrication and characterization of graphene-Ag nanoparticles composites. Wuji Cailiao Xuebao(Journal of Inorganic Materials). 2012;27:89-94.

[81] Biesinger MC, Payne BP, Grosvenor AP, Lau LWM, Gerson AR, Smart RSC. Resolving surface chemical states in XPS analysis of first row transition metals, oxides and hydroxides: Cr, Mn, Fe, Co and Ni. Applied Surface Science. 2011;257:2717-30.

[82] Choi JG, Thompson LT. XPS study of as-prepared and reduced molybdenum oxides. Applied Surface Science. 1996;93:143-9.

[83] Aricò AS, Shukla AK, Kim H, Park S, Min M, Antonucci V. An XPS study on oxidation states of Pt and its alloys with Co and Cr and its relevance to electroreduction of oxygen. Applied Surface Science. 2001;172:33-40.

[84] Li H, Gao Y, Wang C, Yang G. A Simple Electrochemical Route to Access Amorphous Mixed-Metal Hydroxides for Supercapacitor Electrode Materials. Advanced Energy Materials. 2015;5:n/a-n/a.

[85] Hanawa T, Hiromoto S, Asami K. Characterization of the surface oxide film of a Co–Cr–Mo alloy after being located in quasi-biological environments using XPS. Applied Surface Science. 2001;183:68-75.

[86] Zhang G, Li W, Xie K, Yu F, Huang H. A One-Step and Binder-Free Method to Fabricate Hierarchical Nickel-Based Supercapacitor Electrodes with Excellent Performance. Advanced Functional Materials. 2013;23:3675-81.

[87] Eisenberg M, Tobias CW, Wilke CR. Ionic Mass Transfer and Concentration Polarization at Rotating Electrodes. Journal of The Electrochemical Society. 1954;101:306-20.

[88] Lu X, Liu T, Zhai T, Wang G, Yu M, Xie S, et al. Improving the Cycling Stability of Metal–Nitride Supercapacitor Electrodes with a Thin Carbon Shell. Advanced Energy Materials. 2014;4:1300994-n/a.

[89] Zhu J, Xu Z, Lu B. Ultrafine Au nanoparticles decorated NiCo2O4 nanotubes as anode material for high-performance supercapacitor and lithium-ion battery applications. Nano Energy. 2014;7:114-23.

[90] Li T, Li X, Wang Z, Guo H, Li Y. A novel NiCo2O4 anode morphology for lithium-ion batteries. Journal of Materials Chemistry A. 2015;3:11970-5.

[91] Li J, Xiong S, Liu Y, Ju Z, Qian Y. High Electrochemical Performance of Monodisperse NiCo2O4 Mesoporous Microspheres as an Anode Material for Li-Ion Batteries. ACS Applied Materials & Interfaces. 2013;5:981-8.

[92] Yang Y, Wang S, Jiang C, Lu Q, Tang Z, Wang X. Controlled Synthesis of Hollow Co–Mo Mixed Oxide Nanostructures and Their Electrocatalytic and Lithium Storage Properties. Chemistry of Materials. 2016;28:2417-23.

[93] Wang B, Li S, Wu X, Liu J, Tian W. Hierarchical NiMoO4 nanowire arrays supported on macroporous graphene foam as binder-free 3D anodes for high-performance lithium storage. Physical Chemistry Chemical Physics. 2016;18:908-15.

[94] Marino C, Debenedetti A, Fraisse B, Favier F, Monconduit L. Activated-phosphorus as new electrode material for Li-ion batteries. Electrochemistry Communications. 2011;13:346-9.

[95] Wu HB, Pang H, Lou XW. Facile synthesis of mesoporous Ni0.3Co2.7O4 hierarchical structures for high-performance supercapacitors. Energy & Environmental Science. 2013;6:3619-26.

[96] Zhang GQ, Wu HB, Hoster HE, Chan-Park MB, Lou XW. Single-crystalline NiCo2O4 nanoneedle arrays grown on conductive substrates as binder-free electrodes for high-performance supercapacitors. Energy & Environmental Science. 2012;5:9453-6.

ABSTRACT

**NOVEL DESIGN AND SYNTHESIS OF TRANSITION METAL HYDROXIDES AND
OXIDES FOR ENERGY STORAGE DEVICE APPLICATIONS**

by

PEIFENG LI

December 2016

Advisor: Dr. Simon Ng

Major: Materials Science and Engineering

Degree: Master of Science

Supercapacitors (SCs) and Li-ion batteries (LIBs) are two types of important electrical energy storage devices with high power density and high energy density respectively. However, to satisfy the increasing demand of high-performance energy storage devices, the energy density of SCs and power/energy densities of LIBs have to be further improved. The exploration, research, and development of electrode materials with high-performance for applications in SCs and LIBs are still needed to meet the ever-increasing demand on energy and power densities. Herein, the amorphous Ni-Co-Mo ternary hydroxides nanoflakes for SCs and oxides nanoflakes for LIBs with ultrathin structure, abundant open spaces, and interconnecting mesoporous were prepared via electrodeposition method and further annealing process, respectively. The as-obtained materials with unique hierarchical structures offer a large electrochemical active area, resulting in a fast ion transportation (OH^- in SCs and Li^+ in LIBs) electrolyte immersion, as well as provide effective pathways for electron transport. Thus, the as-prepared Ni-Mo-Co triple hydroxides and oxides electrodes exhibit a high specific capacitance /capacity (3074 F g^{-1} at 2 A g^{-1} in SCs and 1132.31 mA h g^{-1} at 0.2 A g^{-1} in LIBs), remarkable rate performance, as well as

long-term cyclability in SCs and LIBs, respectively. Also, the effect of composition of trimetallic hydroxides on SCs performance have been studied, and the performance have been optimized by tuning the feeding ratio of Ni, Mo, and Co. It is found that supreme performance was achieved when feeding ratio Ni/Mo/Co (1/1/0.4).

AUTOBIOGRAPHICAL STATEMENT

I was born in Shanxi province, China in 1992. I lived in Taiyuan city, which is the capital city of Shanxi from birth to 2011, and moved to Shiyan city, Hubei province, China for studying. I received my B.E. degree in Materials Science and Engineering from Hubei University of Automobile Technology (H.U.A.T) in 2014. In August 2014, I enrolled in the Materials Science and Engineering graduate program at Wayne State University (WSU). As a master's student, I joined Dr. Simon Ng's research group in 2015, and choose the thesis plan for my master program. My research mainly focused on novel nano transition hydroxides/ oxides materials for energy storage device applications.